EFFECT OF THERMOMECHANICAL WORKING ON MICROSTRUCTURAL REFINEMENT IN Ti - 6 . 8 Al - 3 . 2 Mo - 1 . 8 Zr - 0 . 3 Si ALLOY

by

VINAYA SHUKLA

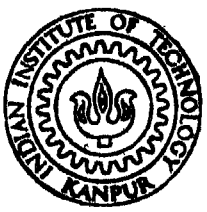

DEPARTMENT OF METALLURGICAL ENGINEERING

INDIAN INSTITUTE OF TECHNOLOGY KANPUR

JULY, 1991

EFFECT OF THERMOMECHANICAL WORKING ON MICROSTRUCTURAL REFINEMENT IN Ti - 6 . 8 Al - 3 . 2 Mo - 1 . 8 Zr - 0 . 3 Si ALLOY

A Thesis Submitted
in Partial Fulfilment of the Requirements
for the Degree of

MASTER OF TECHNOLOGY

by

VINAYA SHUKLA

to the

DEPARTMENT OF METALLURGICAL ENGINEERING
INDIAN INSTITUTE OF TECHNOLOGY KANPUR

JULY, 1991

ME-1991-M-SHU-EFF

CERTIFICATE

It is certified that the work contained in the thesis entitled, "Effect of Thermomechanical Working on Microstructural Refinement in Ti - 6.8 Al - 3.2 Mo - 1.8 Zr - 0.3 Si Alloy" by "Vinaya Shukla" has been carried out under our supervision and that this work has not been submitted elsewhere for a degree.

S Bhargava

Dr. S. Bhargava
Assistant Professor

(On leave)

Dr. R.K. Ray
Professor

Department of Metallurgical Engineering
Indian Institute of Technology , Kanpur

8th July, 1991.

ACKNOWLEDGEMENT

I take this opportunity to thank Dr. S. Bhargava and Dr. R.K. Ray for their guidance and constant encouragement throughout the course of this project. I am grateful to Shri H.C. Srivastava, Shri K.P. Mukherjee, Shri Awasthi, Shri Srivastava, and the workshop staff for their assistance in my experimental work.

Thanks are also due to Shri R.K. Bajpai for helping me with the figures and Sri U.S. Misra for his excellent typing.

VINAYA SHUKLA

CONTENTS

LIST OF TABLES

LIST OF FIGURES

ABSTRACT

A novel technique for obtaining an equiaxed α morphology in Ti-632Si alloy has been suggested. The deformation schedule consists of hot rolling of β quenched and aged structure in the (α+β), β or β and (α+β) temperature field followed by recrystallization annealing in the (α+β) field. Changes occurring in the microstructural features of Ti-632Si alloy at each processing stage were carefully examined. It was found that the lamellar α structure, obtained after water quenching and aging at hot rolling temperature, showed different characteristics at different temperatures and strains. In the (α+β) field, aspect ratio of α lamellae increased with increasing strain and decreasing rolling temperature. Recrystallization annealing of the hot rolled structure gave equiaxed grains of α. Equiaxed microstructure evolution was found to depend on rolling temperature, strain, initial lamellae thickness, and annealing time. Thus equiaxed α grains as small as 1 μm were produced by hot rolling followed by recrystallization annealing. On recrystallization of the β rolled structure, α lamellae were formed whose aspect ratio was found to decrase with increasing strain .

CHAPTER 1

INTRODUCTION

1.1 Specific Properties and Applications of Titanium and its Alloys [1]

Titanium possesses an outstanding combination of physical, chemical and mechanical properties. It is a low density element and can be greatly strengthened by alloying and mechanical working. It is non-magnetic and shows a relatively lower thermal expansion coefficient. Some of the important physical properties of titanium have been shown in Table 1.1.

Ability of titanium and its alloys to passivate provide them a high degree of immunity against a wide range of acidic, alkaline and saline media and thus makes them useful corrosion resistant materials. Similarly, these alloys can be used upto ~ 750K without encountering the problem of their oxidation.

With strength capability almost equal to that of low carbon steels and density nearly half of them titanium alloys can be strengthened to achieve a specific strength (strength per unit weight) equal to that of ultra-high strength steels. The specific fracture toughness (fracture toughness K_{1c}, per unit weight) of titanium alloys, similarly, is superior to most engineering metals and alloys. Most of the titanium alloys developed to date also show an excellent combination of creep and fatigue strength making them well suited for dynamically loaded structural components. Further, most of the dual-phase titanium alloys of the family represented by Ti - 6 Al - 4V can exhibit a high value of strain rate sensitivity approaching to unity which

Table 1.1

Physical Properties of Elemental Titanium

Atomic number	22
Atomic weight	47.90
Atomic volume	10.6 W/D
Covalent radius	1.32 A^{o}
First ionization energy	158 k-cal/g-mole
^Thermal neutron absorption cross-section	5.6 barns/atom
Crystal structure	Alpha: close-packed hexagonal ≤ 1155.5K Beta: body-centered cubic ≥ 1155.5K
Color	Dark grey
Density	4.51 g/cm^{3}
Melting point	1941 ± 10 K
Solidus/liquidus	1998 ± 10 K
Boiling point	3533 K
Specific heat (at 25°C)	0.518 J/kg K
Thermal conductivity	9.0 BTU/hr ft^{2} ^{o}F
Heat of fusion	440 kJ/kg
Heat of vaporization	9.83 MJ/kg
Specific gravity	4.5
Modulus of elasticity	$1.027x10_{9}^{11}$ N/m^{2}
Young's modulus of elasticity	116 x 10^{9} N/m^{2} 102.7 GPa
Poisson's ratio	0.41
Coefficient of friction	0.8 at 40 m/min 0.68 at 300 m/min
Specific resistance	554 uohm-mm
Coefficient of thermal expansion	$8.64x10^{-6}/^{o}C$
Electrical conductivity	3% IACS (copper 100%)
Electrical resistivity	47.8 uohm-cm
Electronegativity	1.5 (Pauling's)
Temperature coefficient of electrical resistance	0.0026/°C
Magnetic susceptibility	$1.25x10^{-6}$
Magnetic susceptibility	3.17 emu/g

puts them among the most desirable candidate materials for superplastic forming/isothermal forging. Selected mechanical properties of a few titanium alloys have been shown in Table 1.2.

Due to the excellent corrosion resistance displayed by titanium and its alloys, they find extensive applications in heat exchangers, reactor vessels, desalination plants and several other components in chemical, marine and petrochemical industries. Its non-toxicity and biocompatibility in addition to excellent corrosion resistance, is made use of in prosthetic devices such as heart-value parts and leg bone replacements or splints. Applications related to corrosion resistance and biocompatible properties account for about 30% of titanium demand and is in general met by unalloyed titanium.

Majority of the demand for titanium alloys, however, is from aerospace industries where high specific strengths make them an attractive choice for air frames, blades and other parts of both low as well as high pressure compressors of turbine engines. Though strength efficiency is the prime consideration for such applications other requirements like fatigue life, fracture toughness, creep, microstructural stability at high temperatures may also have to be met depending on nature of application. To meet these multifarious requirements different alloys have been developed.

1.2 Classification of Titanium Alloys [2]

Pure titanium has two allotropic forms, the low temperature hcp α-phase and the elevated temperature bcc β-phase. Alloying

Table 1.2

Tensile Properties of Selected Alloys

Alloy	Tensile strength (min) (MPa/kg)	Yield stren-gth(min) (MPa/kg)	Elong-ation (%)	Reduction in area (%)	Charpy impact stren-gth (J)	Fatigue streng-th(MPa)	Fracture tough-ness MPa $\sqrt{m}$
Ti-5Al-2.5 Sn (ELI)	807	745	16	--	26	485-495	
Ti-6Al-4V	993 -1172	924 -1103	15	35	19	489-620	32-123
Ti-6Al-2Sn-4Zr-6Mo	1269	1172	10	23	--	620-751	26-34
Ti-13V-11Cr-3 Al	1220	1172	8	--	--	--	--
4340 (Ultra high strength steel)	1965	1482	--	--	--	--	71
Al alloy (20240)	185.495	75-395	13-20	--	--	--	90-140
Mg alloy (A2318)	255-290	150-220	15-21	--	4	--	

Note: Range is provided in certain cases since property values depend on microstructural state. Minimum values are given where range is not specified.

elements added tend to preferentially stabilize one or other of these phases. In pure titanium the transformation from low temperature hcp α-phase to high temperature bcc β-phase occurs at 1155.5 K.

Elements like Al, C, O, N, Sn, etc. when added to titanium raise the transformation temperature (commonly referred to as β-transus temperature) of the alloy and thus stabilize the alpha phases to a temperature higher than 1155.5 K. These elements are referred to as α stabilizes. Potency of these elements for stabilizing the α-phase, however, is different. Rosenberg has suggested the following expression for computing the aluminium equivalent Al^* of the alloy.

$$Al^* = Al + \frac{Sn}{3} + \frac{Zr}{6} + 10\,(O + C + 2N) \quad wt\%$$

Elements like Mo, V, Nb, Ni, Mn, Cu, Cr, Fe, H, Si etc. when added to the alloy, lower the β-transus temperature and hence are characterised as β stabilizers.

Variation of β transus temperature with the percentage of alloying additions can be obtained from phase diagrams. Schematic phase diagrams for Ti-α stabilizes and Ti-β stabilizers (isomorphous) have been shown in Figure 1.1. Thus the type and concentration of alloying elements determines the equilibrium concentration which forms the basis for classification of titanium alloys. Depending on the type of alloying addition made, titanium alloys can be alpha, near-alpha, alpha-beta, near beta or beta alloys.

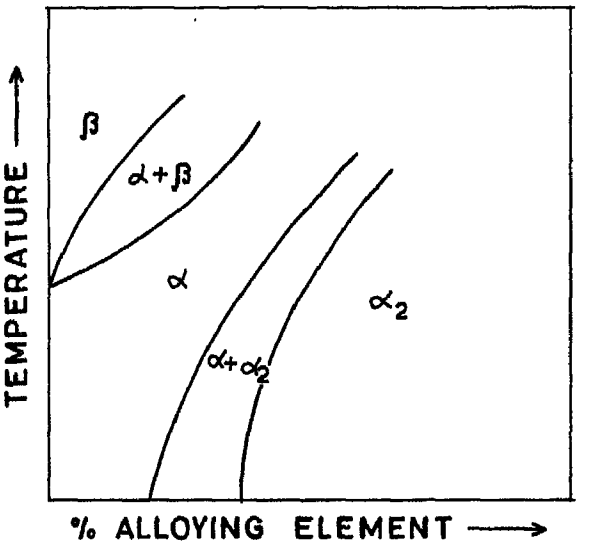

(a) α - STABILIZED

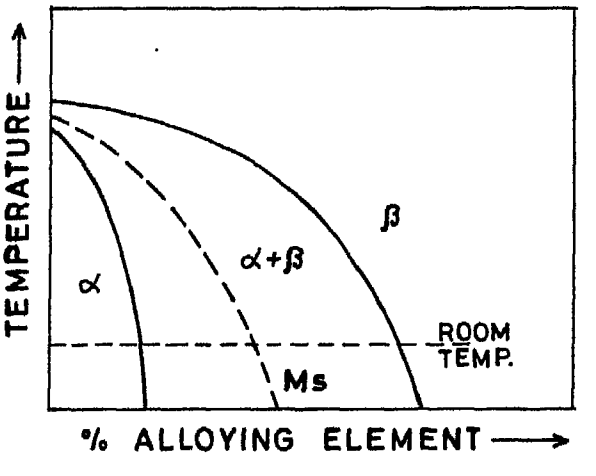

(b) β - STABILIZED

Fig.1.1 Schematic phase diagram of binary Ti alloy systems.

1.2.1 Alpha Alloys

These alloys contain only alpha stabilizers as alloying elements and hence the room temperature microstructure consists of hcp α-phase only. Due to the single phase nature of these alloys no microstructural strengthening can be achieved in them. Solid solution strengthening of them is also limited because an aluminium equivalent Al^* of more than 9.0 promotes the formation of the brittle phase, α_2. Thus, these relatively lower strength titanium alloys have limited scope of heat treatment but due to the absence of β-phase in their microstructure, have better microstructure stability and weldability. These alloys however have poor workability. Examples of these alloys are Cp Ti and Ti - 5 Al - 2.5 Sn, both of which find significant commercial applications.

1.2.2 Near Alpha Alloys

Small additions 1-2 wt% of beta stabilizers to alpha alloys give rise to near alpha alloys. By such additions problems related to low strength and poor hot workability of high aluminium compositions are eliminated and a compromise is effected between the higher strength which is available with alpha-beta alloys and better high temperature stability and weldability which are characteristics of alpha alloys. Examples of these alloys are Ti - 11 Sn - 2.25 Al - 5 Zr - 1 Mo - 0.25 Si, Ti - 6 Al - 2 Sn - 4 Zr - 2 Mo - 0.1 Si, Ti - 6 Al - 5 Zr - 0.5 Mo - 0.3 Si all of which find applications in turbine engine components.

1.2.3 Alpha Beta Alloys

Somewhat higher additions of β stabilizers (4-6%) in titanium alloys stabilizes small volume fraction of β phase in the microstructure [See phase diagram in Figure 1.1(b)]. Morphology of the two phases present in such dual phase alloys can be considerably varied by controlling various heat treatment and mechanical working parameters. A wide range of different property levels can therefore be achieved in these alloys. Ti - 6 Al - 4V alloy, which is the main alloy of this family, is considered to be the 'trading horse' of the titanium industry. Other important alloys of this family are Ti - 4 Al - 4 Mo - 2 Sn - 0.5 Si, Ti - 6 Al - 6V - 2 Sn, Ti - 6.5 Al - 3 Mo - 2 Zr - 0.3 Si. All these alloys find extensive applications in the aerospace industry.

1.2.4 Near Beta Alloys

Still larger additions of beta stabilizers can cause retention of beta phase at room temperature. Therefore, near beta alloys are also known as metastable beta alloys. These alloys show excellent cold formability in which high strengths can also be achieved through proper heat treatment. Examples of these alloys are Ti - 13V - 11 Cr - 3 Al, Ti - 11.5 Mo - 6 Zr - 4.5 Sn, Ti - 10V - 2 Fe - 3 Al. This alloy family has emerged for commercial applications only in the recent past.

1.2.5 Beta Alloys

These alloys contain very large amounts of beta stabilizers which gives them high densities, poor ductilities, poor oxidation resistance and therefore little commercial value. Ti-Nb alloys come under this category. These alloys can be used as low temperature superconductors but their commercial importance is not very high. In the vocabulary of titanium industry therefore, near-β titanium alloys are referred to as beta alloys.

Since the present study is concerned with an alpha-beta type of alloy the discussion given below will be confined only to this family of titanium alloys.

1.3 Importance of Alpha-Beta Alloys

Alpha-Beta alloys have been designed to combine the better part of properties of both alpha and near-beta alloys. Because of the dual phase structure consisting of alpha and beta phases, a wide range of microstructural features, varying in size and morphology of both the constituent phases can be obtained in them. Since the rule of mixtures is not followed by them [3], a considerable amount of 'microstructural strengthening' can be imparted to them. Thus for the same alloy it is possible to have a wide range of property levels by altering the morphology and size of its microstructural constituents. 0.2% yield strength, tensile strength and ductility do not get influenced very much by the manipulation of the microstructure but properties involving dynamic loading such as fracture toughness, fatigue strength, fatigue crack propagation rate (FCP) get influenced by microstructural changes to a very large degree. Similarly creep

resistance and stress rupture strength are known to vary drastically with the microstructural state of the material.

1.4 Microstructural Control in Alpha-Beta Alloys

Microstructures are characterised by the nature of phases present, their shape, size, morphology which in turn are functions of heat treatment and working schedule. Before we go into details lets look at some of the prominent microstructural features in titanium alloys.

1.4.1 Microstructural Features

(a) Primary Alpha (α_p) - It refers to the alpha phase in a crystallographic structure that is retained from the last high temperature ($\alpha+\beta$) working or heat treatment. Morphology of primary α is influenced by prior thermomechanical history and may vary from lamellar to equiaxed grains.

(b) Alpha Prime (α') - A supersaturated non-equilibrium hexagonal alpha phase formed by a diffusionless transformation of the beta phase. It occurs as fine, randomly oriented needles.

(c) Secondary Alpha - Alpha phase generated from alpha prime on reheating in two phase field is designated as secondary alpha. It shows lamellar structure whose dimensions are function of temperature and time of heating.

(d) Grain Boundary Alpha - Primary alpha outlining prior beta grain boundaries are referred to as grain boundary alpha.

It evolves by heterogeneous transformation when cooled slowly from the beta to the alpha-beta phase field.Thickness and continuity of the layer depends on cooling rate and alloy composition.

(e) Alpha Double Prime (α'') - It refers to a supersaturated, non-equilibrium orthorhombic phase formed by diffusionless transformation of the beta phase in certain alloys like Ti-Mo, Ti-Nb etc. which have high concentration of beta stabilizers.

(f) Metastable Beta - Refers to the beta phase which is retained at room temperature instead of undergoing martensitic transformation. Prior beta grain boundaries are visible whose sizes are function of temperature and time of solutionizing in the beta phase field.

(g) Alpha (α_2) - Refers to the ordered alpha phase Ti_3Al produced by segregation of alloying elements and existing as small precipitates.

(h) Silicides - In high silicon bearing alloys silicon combines with titanium and other alloying elements to form complex compounds known as silicides e.g. Ti_5Si_3, Ti-Mo-Si etc. which exist as precipitates in the matrix.

1.4.2 Effect of Heat Treatment On Microstructure

Heat treatment of titanium alloys are done for a variety of reasons - to reduce residual stresses known as stress relieving, generate acceptable combination of ductility, machinability and dimensional and structural stability known as annealing, to increase strength and optimise special properties

such as fracture toughness, fatigue strength, creep strength etc. The latter requirements are met by proper choice of thermal cycling to generate microstructures yielding requisite properties. The basis for microstructural manipulation during heat treatment of titanium alloys centres around the beta-alpha phase transformation which takes place in these alloys during cooling. Transformation can occur either by nucleation and growth mechanism yielding Widmanstatten structure or martensitically depending on alloy composition and cooling rate [1,4,5,6]. Figure 1.2 gives a schematic representation of the continuous cooling transformation diagram of an $\alpha + \beta$ titanium alloy.

When the alloy is slowly cooled below the beta transus alpha begins to nucleate at beta grain boundaries with a crystallographic Burgers orientation relationship

$$(0001)_\alpha \;||\; \{0\,1\,1\}_\beta$$
$$\langle 11\bar{2}0\rangle_\alpha \;||\; \langle 1\,1\,1\rangle_\beta$$

Because of the close atomic matching along this common nucleation plane, the alpha phase thicknes relatively slowly perpendicular to it but grows faster along it leading to plate like structure. A schematic illustration of the formation of Widmanstatten structure is shown in the Figure 1.3. Even when cooling at rates when nucleation and growth mechanism is operative morphology of the alpha phase is influenced by alloy content and cooling rates for e.g. during slow cooling (or in alloys learner is beta stabilizer) the Widmanstatten alpha plates form in colonies or packets of plates all of which belong to the

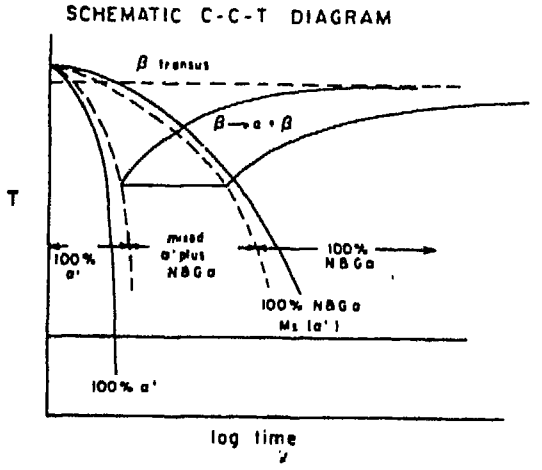

Fig. 1.2 Schematic CCT diagram showing the effect of cooling rate on the constitution of an (α + β) Ti alloy

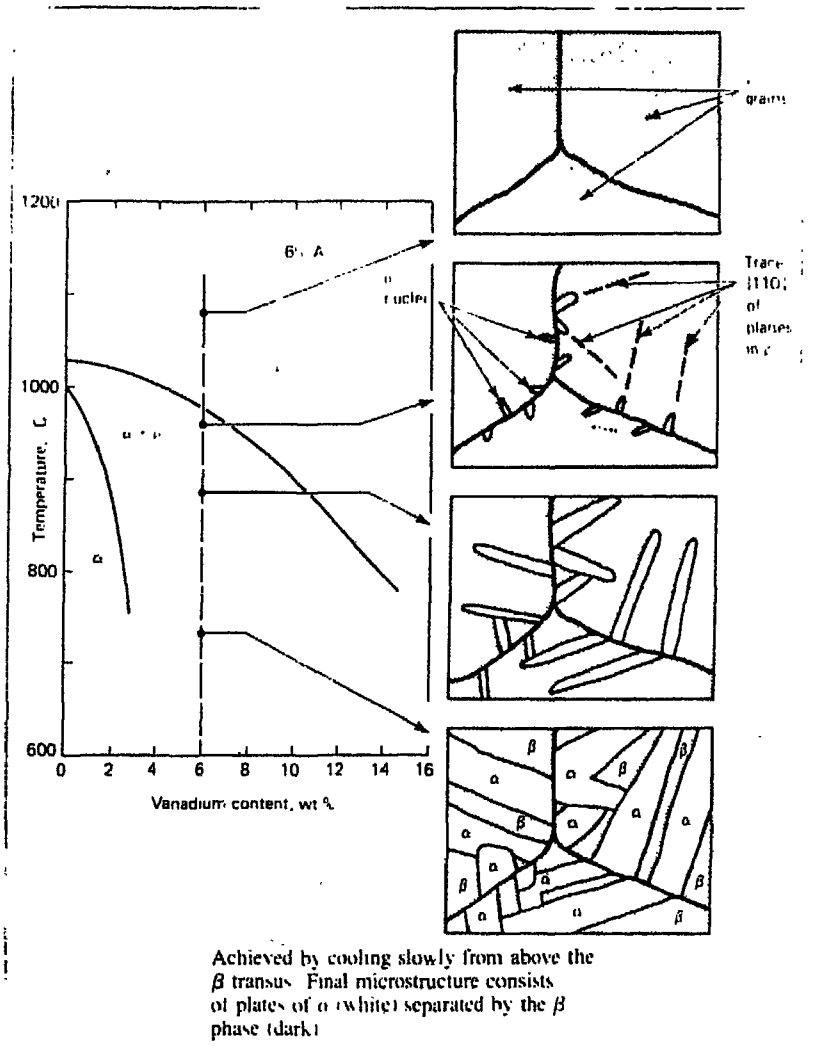

Achieved by cooling slowly from above the β transus. Final microstructure consists of plates of α (white) separated by the β phase (dark).

Fig. 1.3 Schematic illustration of formation of Widmanstatten structure in Ti-6Al-4V alloy

same variant of the orientation relationship between the alpha and beta phases. With increase in cooling rates or increase in beta stabilizers content nucleation of additional variants become more prevalent and the number of plates in the Widmanstatten alpha decreases until a point is reached when the transformed region consists of a random mixture of α-plates belonging to different variants of the orientation relationsip (Figure 1.4).

Rapid quenching from the beta phase field leads to formation of randomly oriented needle shaped martensite (α')which is supersaturated with beta stabilizing elements like Mo and V. Increasing beta stabilizer content not only shifts the C curve for N & G transformation to the right leading to evolution of α' at lower cooling rates but also depresses the M_f (Martensite finish temperature) the latter causing incomplete transformation resulting in some metastable beta being found at room temperature. Subsequent aging of martensite leads to nucleation of beta phase at plate boundaries and internal substructures (such as twins) [7] followed by growth. Diffusion of excess beta-stabilizing elements from supersaturatd α' is utilized during growth with the latter gradually transforming to equilibrium α [8]. Resulting fine lamellar or acicular alpha shows superior creep properties and higher fracture toughness values [9,10,11].

Phase transformations discussed above form the basis for various heat treatment practices followed industrially a summary of which is given in Table 1.3.

A wider range of microstructures can be produced by a combination of heat treatment and mechanical working than is

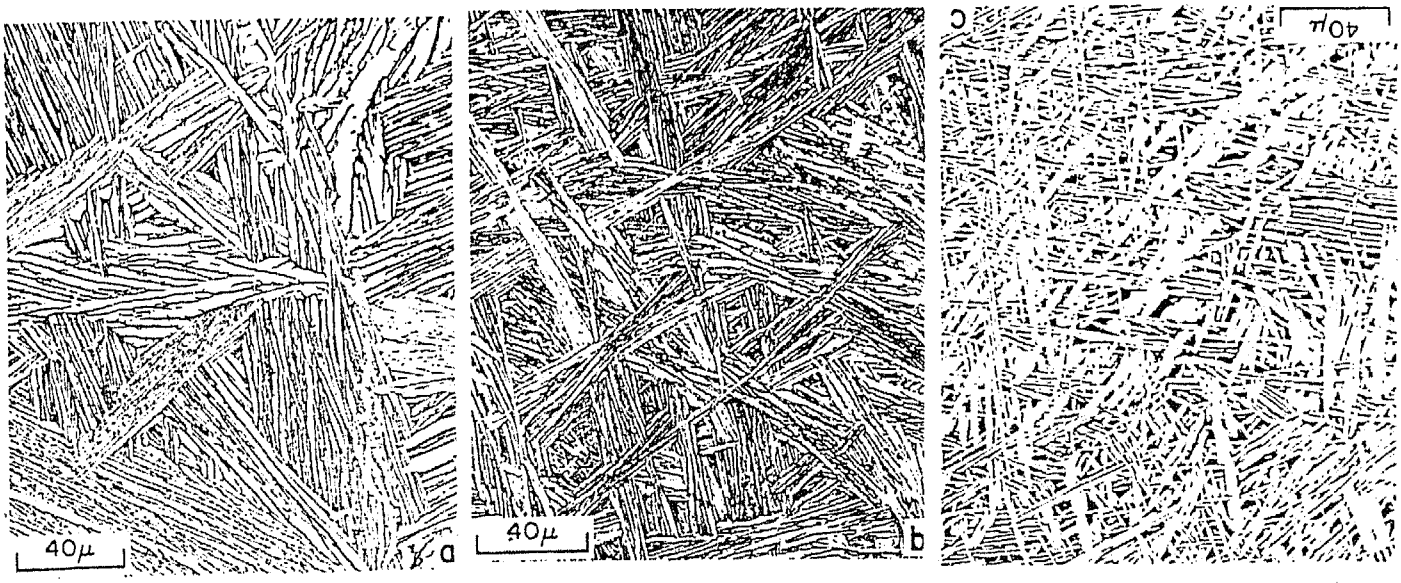

Fig. 1.4 Microstructural illustration of effect of β-stabilizing alloying elements on size and distribution of α-phase packets in β-processed materials (a) Ti-6-4 (b) Ti-6-6-2 (c) Ti-6-2-4-6

Table 1.3 Summary of Heat Treatments for (α +β) Ti Alloys

Heat treatment designation	Heat treatment cycle	Microstructure
Duplex anneal (DA)	Solution treat at 50-75°C below T_B(a), air cool and age for 2-8 h at 540-675°C	Primary α, plus Widmanstätten α + β regions
Solution treat and age (STA)	Solution treat at ~40°C below T_B, water quench(b) and age for 2-8 h at 535-675°C	Primary α, plus tempered α' or a β + α mixture
Beta anneal (BA)	Solution treat at ~15°C above T_B, air cool and stabilize at 650-760°C for 2 h	Widmanstätten α + β colony microstructure
Beta quench (BQ)	Solution treat at ~15°C above T_B, water quench and temper at 650-760°C for 2 h	Tempered α
Recrystallization anneal (RA)	925°C for 4 h, cool at 50°C/h to 760°C, air cool	Equiaxed α with β at grain-boundary triple points
Mill anneal	α + β hot work + anneal at 705°C for 30 min to several hours and air cool	Incompletely recrystallized α with a small volume fraction of small β particles

(a) T_B is the β-transus temperature for the particular alloy in question. (b) In more heavily β-stabilized alloys such asTi-6Al-2Sn-4Zr-6Mo or Ti-6Al-6V-2Sn, solution treatment is followed by air cooling. Subsequent aging causes precipitation of α phase to form an α + β mixture.

possible through heat treatment alone [12]. Development of equiaxed alpha as one of the constituent phases form the basis of most of them as it shows clear advantages over lamellar structures in certain properties such as higher strengths, ductility and formability [13,14], better hydrogen tolerance and low cycle fatigue properties [3,15,16]. Thus both fabrication as well as microstructural evolution can be effected by proper control of deformation parameters during high temperature working - a process known as thermomechanical treatment [5].

1.4.3 Effect of Hot Working on Microstructure

Deformations of alpha-beta alloys is governed by the deformation characteristics of the difficult to deform hcp alpha phase. Deformation takes place by both slip and twinning though contribution of the latter is low [17,18]. Lamellar alpha phase elongate and strain harden on working along with formation of sub-boundaries and shear bands, the misorientation of which increases with increasing degree of working [19]. Higher degree of working leads to fracturing of lamellae into small aspect ratio alpha grains [20]. Subsequent break-up to equiaxed morphology occurs during annealing when the beta phase penetrates across the lamellar width along the sub-boundaries or shear bands [19,21]. Nature of the starting microstructure characterised by lamellae width therefore affects the evolution of microstructures [18,22]. Other variables like strain [19-23], strain rate [3,17,23,24], temperature [3,17,20,22,23,24],number of passes [22-23] determine amount of stored energy for static recovery and recrystallization processes which also play an important role in

evolution of microstructure during annealing. Kinetics of the dynamics softening mechanisms operative which determine the amount of stored energy is governed by these variables. Alpha-beta alloys soften by dynamic recovery and recrystallization as seen by the nature of the stress strain curve and electron microscopy observations [3,24,26,27].

Hot working can be done by either forging or rolling but the latter is preferred since it leads to alignment of grains along preferred orientations which can be made use of to get better tensile properties along certain directions.

1.5 Texture Development

Ti alloys show strong textures which produce pronounced anisotropies in mechanical properties primarily due to lower crystallographic symmetry of hcp alpha Ti. By proper control of deformation variables texture as a means of strengthening can be utilized to fabricate components having higher strengths along particular directions. Table (1.4) gives the mechanical properties of textured Ti-Al-2Sn-4Zr-6Mo plate in different directions. Different factors that affect texture development are:-

i) Starting microstructure [18]

ii) Rolling temperature [13,20,28,29]

iii) Rolling direction [13]

iv) Reduction in thickness [20,29]

v) Heat treatment [20,29]

vi) Impurity content [30]

vii) Alloy composition [20]

Table 1.4 Effect of Test Direction on Mechanical Properties of Textured Ti Alloy Plate

Test direction (a)	Tensile strength MPa	Yield strength MPa	Elongation, %	Reduction in area, %	Elastic modulus, GPa	K_{Ic} MPa·m$^{1/2}$	K_{Ic} ksi·in.$^{1/2}$	K_{Ic} specimen orientation (b)
L	1027	952	11.5	18.0	107	75	68	L-T
T	1358	1200	11.3	13.5	134	91	83	L-T
S	938	924	6.5	26.0	104	49	45	S-T

(a) High basal pole intensitites reported in the transverse direction, 90° from normal, and also intensity nodes in positions

(b) 45° from the longitudinal (rolling) direction and about 40° from the plate normal. L=longitudinal; T=transverse

Studies on texture are based on the Pole Figure Method which describe statistical distribution of grain orientations using a stereographic plot to depict the spatial distribution of the poles of a particular crystallographic plane. For titanium and its alloys texture representation using pole figures is done by showing distribution of the poles of the basal plane (0001) and the prism plane $(10\bar{1}0)$ the latter to complete the description since former shows a rotational symmetry [5]. Figure 1.5 gives a schematic representation of commonly observed basal and prism plane pole figures for α - Ti. Schematic representation of the effect of temperature and working mode on texture development is shown in Figure 1.6.

1.6 Aims of the Present Study

Titanium alloys possess numerous superior properties but they also have one major drawback which is responsible for limiting their application base. They have low ductility and high elastic spring-back which makes them a difficult metal to work with leading to increase in costs. This problem can be eliminated by applying superplasticity concepts in fabrication. Prime microstructural requirements for superplastic forming in titanium as for other alloys is a uniform,fine grain equiaxed structure which is metallurgically stable at high temperatures. Despite the importance of such a morphology no systematic work has been done to trace and understand its evolution. The objective of the present work was to carry out such a study on the alloy Ti-6.8Al-3.2Mo-1.8Zr-0.3Si which though superior to Ti-6Al-4V in certain respects , has not been much investigated.

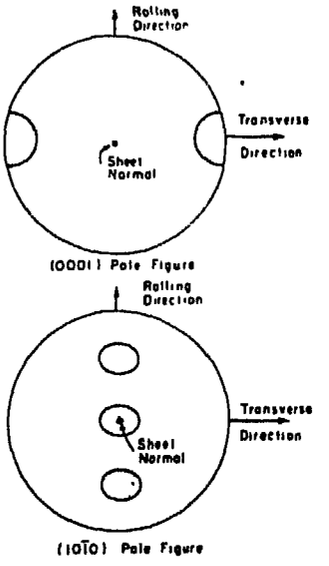

Fig. 1.5 Schematic representation of commonly observed basal and prism plane pole figures for α - Ti

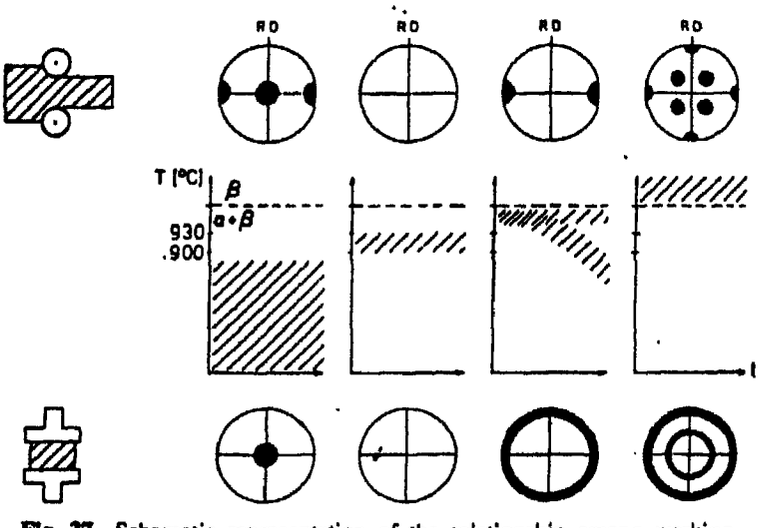

Fig. 37. Schematic representation of the relationship among working method (rolling at top, axisymmetric at bottom), working temperature and texture for Ti-6Al-4V.

Fig. 1.6 Schematic representation of the relationship among working method, working temperature and texture for Ti-6Al-4V alloy

CHAPTER 2

EXPERIMENTAL PROCEDURE

2.1 Raw Material

Ti - 6.5Al - 3.2 Mo - 1.8 Zr - 0.3 Si alloy (hereafter referred to as Ti - 632 Si alloy) used in this study was supplied by Mishra Dhatu Nigam Ltd. Hyderabad. The supplied material was in the form of forged bar of square cross-section of 100 x 100 mm^2. These bars were produced from an ingot which was made from titanium sponge and other master alloys by the vacuum melting of consumable electrode in the vacuum arc remelting (VAR) furnace. Double melting method for preparing the ingot was followed. Ingots thus produced were surface machined and were subsequently forged above the β transus temperature on a hydraulic press of 1500 T capacity. Chemical composition of the supplied material has been shown in Table 2.1. Beta transus temperature of the supplied material as determined by the supplier was $1010^{o}C$.

TABLE 2.1

Alloying Element	Al	Zr	Mo	Si	Fe	O	H	C	N
Amount (wt %)	6.05	1.94	3.44	0.23	0.155	574 ppm	21 ppm	0.014	124 ppm

2.2 Preparation of Blanks for Hot Rolling:

Samples of approximately 37 mm x 14 mm x 4.5 mm were cut from the sheet on a DoAll machine having a vertical cutter. The samples were cooled periodically in running water during cutting to mimimise pick up of oxygen and nitrogen due to their overheating. Samples were thereafter levelled on a belt grinder to make their thickness uniform throughout the cross section of the sample. During surface grinding operation samples were again cooled intermittently in running water.

2.3 Hot Rolling of the Ti - 632 Si Sheets

2.3.1 Heat Treatment Prior to Rolling

As discussed in section 1.4.2 α phase in $(\alpha+\beta)$ alloys of titanium, when cooled from the single phase β field, transformation of the structure can occur either by nucleation and growth or martensitically. While nucleation and growth mechanism gives rise to the Widmanstatten morphology consisting of plate-like α phase the martensitic transformation after aging provides fine lamellar/acicular structure. The conventional practice for obtaining typical $(\alpha+\beta)$ structure is to deform the Widmanstatten structure in the two phase field. The resulting microstructure, though having the primary α in the equiaxed morphology, is normally coarse. In contrast, the present study utilized the fine lamellar structure, obtained by martensitic transformation followed by aging, to achieve the microstructural refinement in Ti-632Si alloy by its thermomechanical working. Therefore all the samples were heated at 1050^{0}C (40^{0}C above the β transus temperature of the alloy) for

20 min and were quenched in water prior to hot rolling. These samples when heated prior to their hot rolling gave the required lamellar structure.

2.3.2 Thermomechanical Treatment

The β quenched samples were heated at the rolling temperature for 20 minutes and then rolled to different thickness reductions in a number of passes. Details of the thermomechanical working schedule are shown in Table 2.2. Preheating was done in a specially designed furnace made of Inconel tube which was having a constant temperature zone of 15 mm.Samples were heated under argon atmosphere. Hot rolling was done on a 2-high rolling mill having 135 mm diameter rolls rotating at a speed of 55 rpm. Rolls were not preheated .The loss in temperature during rolling was compensated by heating for around 2 minutes in between passes. All the hot rolled samples were immediately water quenched (within 5 sec) after the final pass. Schematic diagrams of the heat treatment and deformation sequences followed are shown in Figure 2.1.

2.4 Heat Treatment

Rolled samples were encapsulated in quartz tube under vacuum (0.004 Torr) and heat treated in a horizontal muffle furnace having temperature variation of $\pm$ 5^{o}C. Heat treatment was done for 1 hr and 12 hrs and samples were immediately water quenched.

TABLE 2.2

Sample No.	Rolling Temperature (^{o}C)	% Thickness Reduction	Number of Passes
1	750	47	4
2	750	68	6
3	850	20	2
4	850	45	4
5	850	58	5
6	950	45	3
7	950	60	4
8	1050	20	1
9	1050	35	2
10	1050	46	3
11	1050	59	4
12	1050	22	2
	850	36	3
13	1050	40	3
	850	15	1

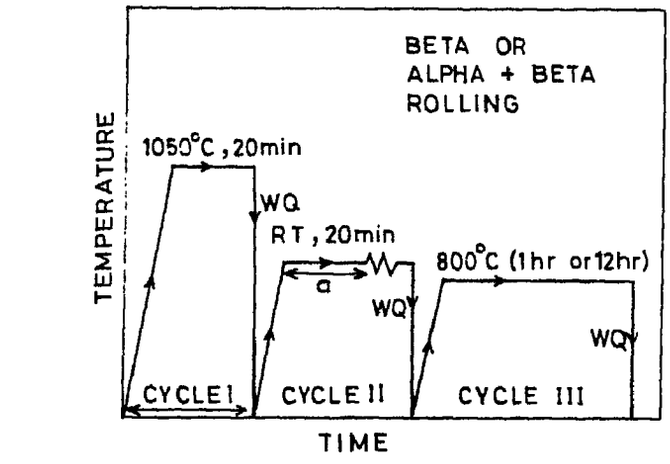

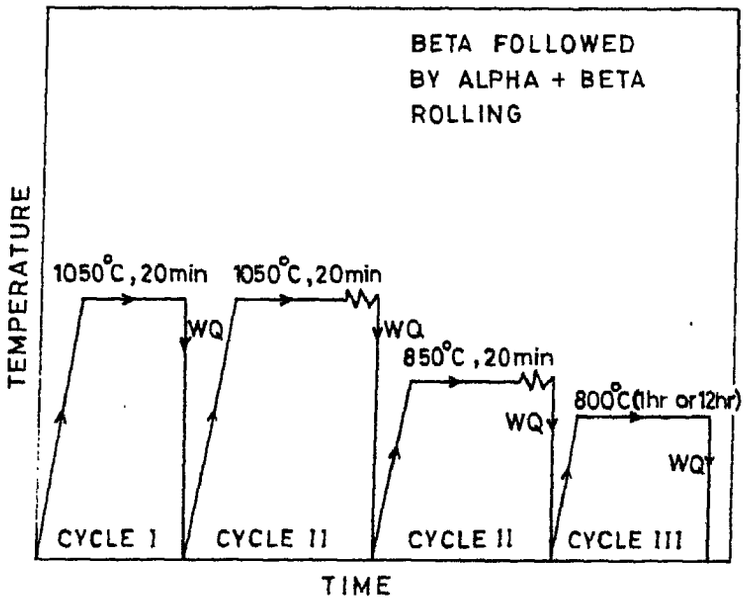

Fig. 2.1 Heat treatment and deformation sequences applied to Ti-632 Si sheets. The three cycles present(1) formation of starting microstructure,(2) deformation conditions and (3) RA treatment

2.5 Microscopy

In order to study the structural charges associated with hot rolling and recrystallization specimens were prepared for microstructural examination by Optical Microscopy, Scanning Electron Microscopy (SEM) and Transmission Electron Microscopy (TEM). Experimental procedures adopted for these purposes are described below.

2.5.1 Optical Microscopy

Metallography samples were cut with the observation plane parallel to the rolling direction and mechanically polished by standard methods to achieve optimum polished surface. Etching was done using Kroll's reagent (95 ml water, 3 ml HNO_3 and 2 ml HF) for 3-5 sec. Samples were thereafter washed, dried and observed under a Lietz Metallux 3 microscope at different magnifications.

2.5.2 Quantitative Microscopy

For determining aspect ratio, length and thickness measurements on more than 75 individual alpha plates were made for each condition Aspect ratio which is a measure of shape is defined as

$$\phi = l/t$$

where l = length and t = thickness

Average aspect ratio $\bar{\phi} = \frac{1}{n} \sum_{i=1}^{n} \frac{l_i}{t_i}$.

In the metallographic cross sections it was not possible to distinguish between width and thickness, due to random sectioning of the alpha plates. The reported t values in this work are the average section thickness. The l measurements are actually section lengths since the angle of plate inclination to the metallographic surface could not be determined.

For determining grain sizes,diameter of individual grains were measured along perpendicular directions and averaged. About 20-25 measurements were made for each condition.

2.5.3 Scanning Electron Microscopy

Certain samples were observed using SEM primarily for quantitative microscopy measurements. Observations were made at 20 kV. Because of etching problems observation could not be made for many samples.

2.5.4 Transmission Electron Microscopy

Specimens were mechanically thinned down to about 60 microns. Then discs of 3 mm diameter were punched out. The discs were electrojet polished in a double jet polisher (Fishione Apparatus) using standard electropolishing techniques [30]. The electrolyte used consisted of 90 ml perchloric acid, 52 ml butanol and 900 ml methanol, the temperature was - 40^{o}C and the voltage 30 V.

After jet polishing the specimen were observed in the EM 301 S transmission electron microscope (Philips make) at 100 kV.

CHAPTER 3

EXPERIMENTAL RESULTS

As mentioned in Chapter 2, the β transus temperature of the as-received material of Ti-6.8 Al-3 Mo-2 Zr - 0.3 Si (designated in this report as Ti - 632 Si alloy) was found to be 1010°C ((1283 K). In order to study the refinement of the microstructural features of the alloy vis-a-vis its thermomechanical working schedule, three batches of the material were prepared and subjected to the following rolling schedule;

i) Rolling in two phases ($\alpha + \beta$) field, i.e. below 1010°C,

ii) Rolling in single phase β field, i.e. above 1010°C,

iii) Rolling in single phase β field followed by rolling in two phase ($\alpha + \beta$) field.

Rolled samples thus obtained were subsequently annealed at 800°C (1073 K) for two time intervals namely 1 hr (3.6 ks) and 12 hrs (43.2 ks). Results obtained by these experiments have been described in this chapter.

3.1 Rolling in Two Phase ($\alpha + \beta$) Field

In order to understand the effect of deformation temperature and strain on the microstructural refinement in Ti - 632 Si alloy in ($\alpha + \beta$) phase field sheet samples were rolled 50°C, 150°C, 250°C and 350°C below its β transus temperature, i.e. at 950°C, 850°C, 750°C and 650°C respectively. However, it was found that the alloy had very poor workability at 650°C and attempts to roll

the samples by imparting even small strains caused severe cracking in them. Rolling experiments at 650°C were therefore not carried out any further.

3.1.1 Starting Microstructures Prior to Their Rolling

A reference to phase diagram of (α + β) alloys of titanium [Figure 1.1 (b)] shows that the volume fraction of α phase decreases with increase in temperature in the (α + β) phase field. As mentioned earlier, all the samples prior to rolling were heated above the β transus temperature and were subsequently quenched in water. Such a treatment gave rise to their martensitic transformation. It was this structure which was preheated to rolling temperatures, i.e. to 750°C, 850°C and 950°C for a period of 20 min (1.8 ks). If such a material is air-cooled after its preheating at rolling temperatures, growth of secondary α occurs masking the morphological features of primary α present in the structure prior to rolling. In order to study the morphology of primary α in pre-rolled samples, therefore, the preheated samples were quenched in water.

Figure 3.1 shows microstructures of water-quenched samples preheated at 950°C, 850°C and 750°C. Randomly oriented thin alpha lamellae having high aspect ratios can be observed in all the three microstructures. It is well understood that nucleation and growth of β phase at martensite (α') plate boundaries leading to its gradual transformation to alpha is responsible for the fine lamellar morphology observed (22,25). Preheating at 850°C which constituted the starting microstructure for rolling at 850°C, as shown in Figure 3.1(b), resulted in increase of

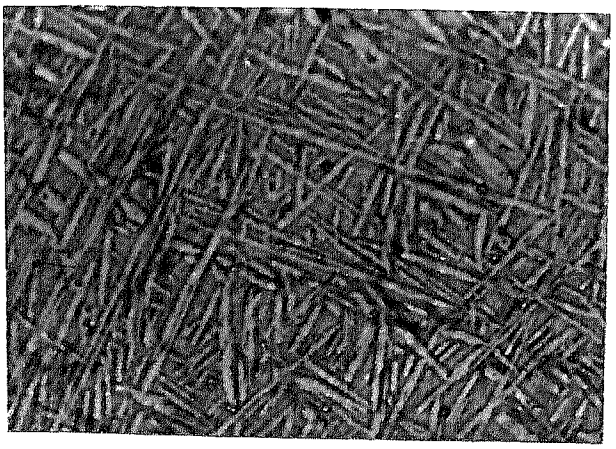

1000 X

a

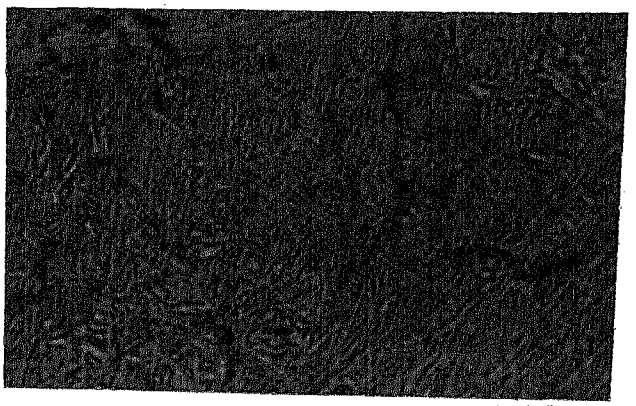

1000 X

b

1000 X

c

Fig. 3.1 Starting microstructures of samples before rolling at different temperatures (a) 950°C, (b) 850°C, (c) 750°C

lamellae thickness due to coarsening accompanied with decrease in volume fraction of alpha phase to around 50%. Annealing at still higher temperatures, i.e. at 950°C resulted in further decrease of volume fraction of alpha phase to 38% and excessive coarsening because of high diffusion rate which increases exponentially with temperature. Microstructures of samples preheated at 950°C [Figure 3.1(a)] also shows diffuse lamellae, edges and striations, the latter arising because of non-uniform growth in the transverse direction. Small annealing times (20 min) could not eliminate them which act as high surface energy reservoirs. Kinks are also observed where lamellae overlap each other in order to satisfy surface tension considerations.

3.1.2 Effect of Hot Rolling Temperature and Strain on as-rolled Microstructure

Hot working temperature affects both the volume fraction as well as nature of starting microstructures which in turn affects the deformation characteristics. Just below the β transus temperature higher volume fraction of softer beta (bcc) phase in combination with accelerated dynamic restoration processes operative at such temperatures, leads to accommodation of strains arising during deformation resulting in predominantly uniform deformation of alpha phase though at certain locations deformation bands originating from localized straining are observed. Figure 3.2 shows the microstructures of samples deformed at 950°C to thickness reductions of 45% and 60% respectively. It can be seen that increasing the degree of deformation leads to increasing lengths and fineness of the

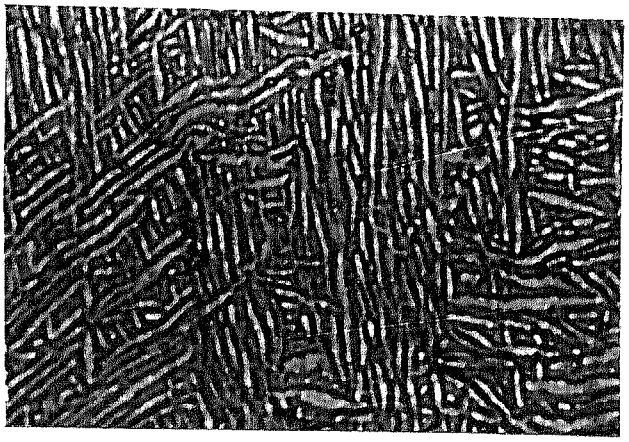

1000x

a

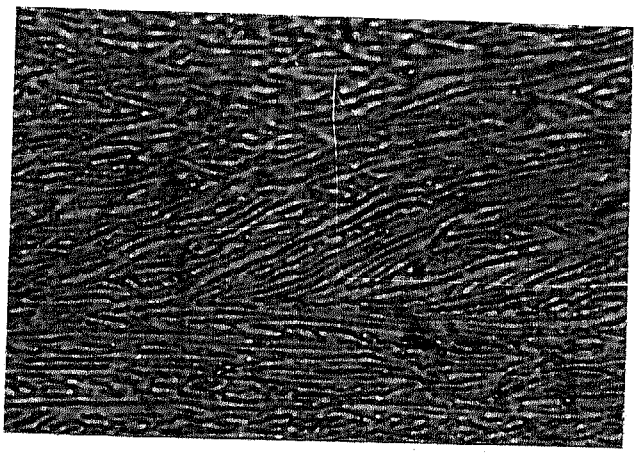

1000x

b

Fig. 3.2 Microstructures of samples rolled at 950°C with different thickness reductions (a) 45%, (b) 60%

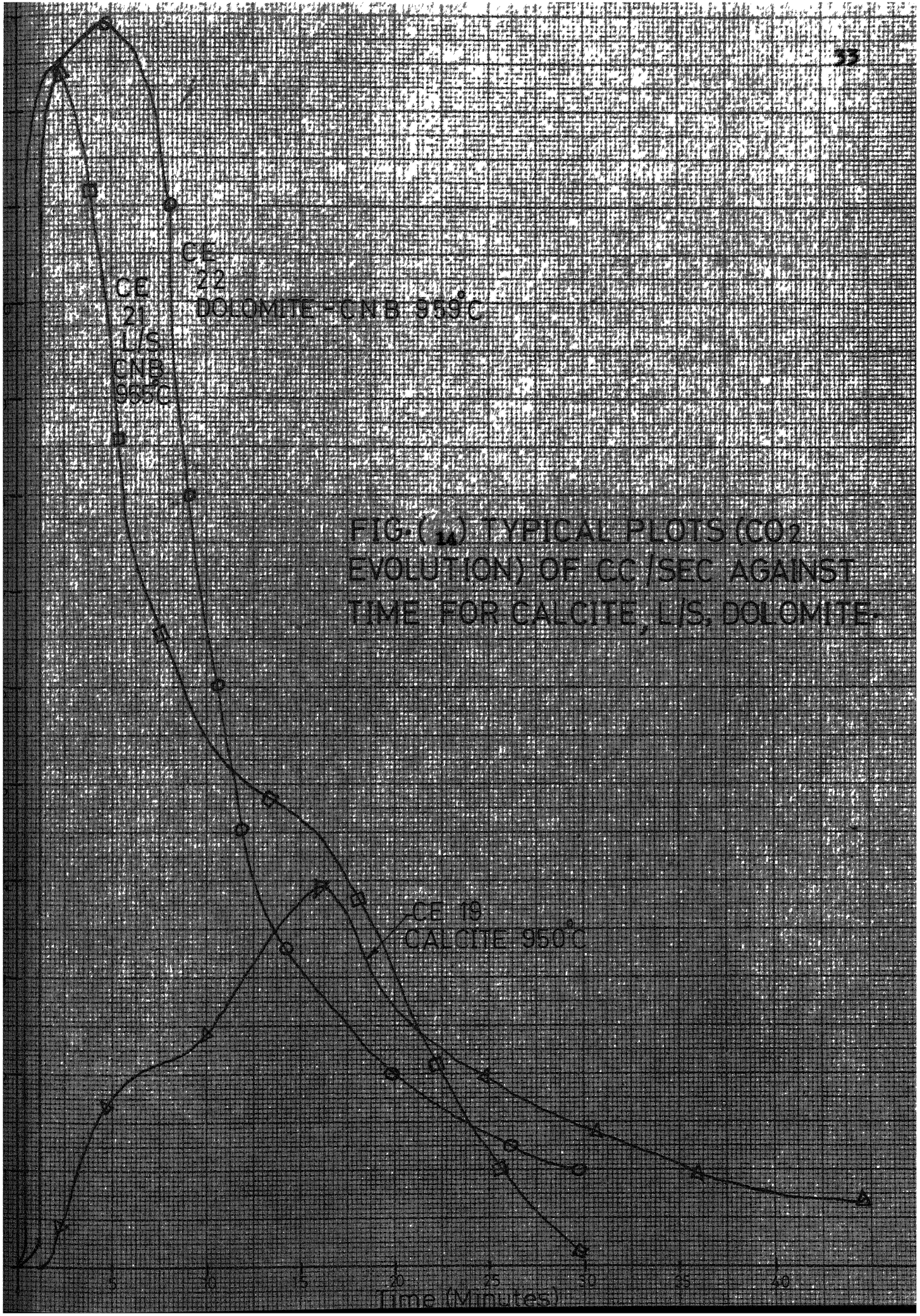

FIG. (14) TYPICAL PLOTS (CO_2 EVOLUTION) OF CC/SEC AGAINST TIME FOR CALCITE, L/S, DOLOMITE-

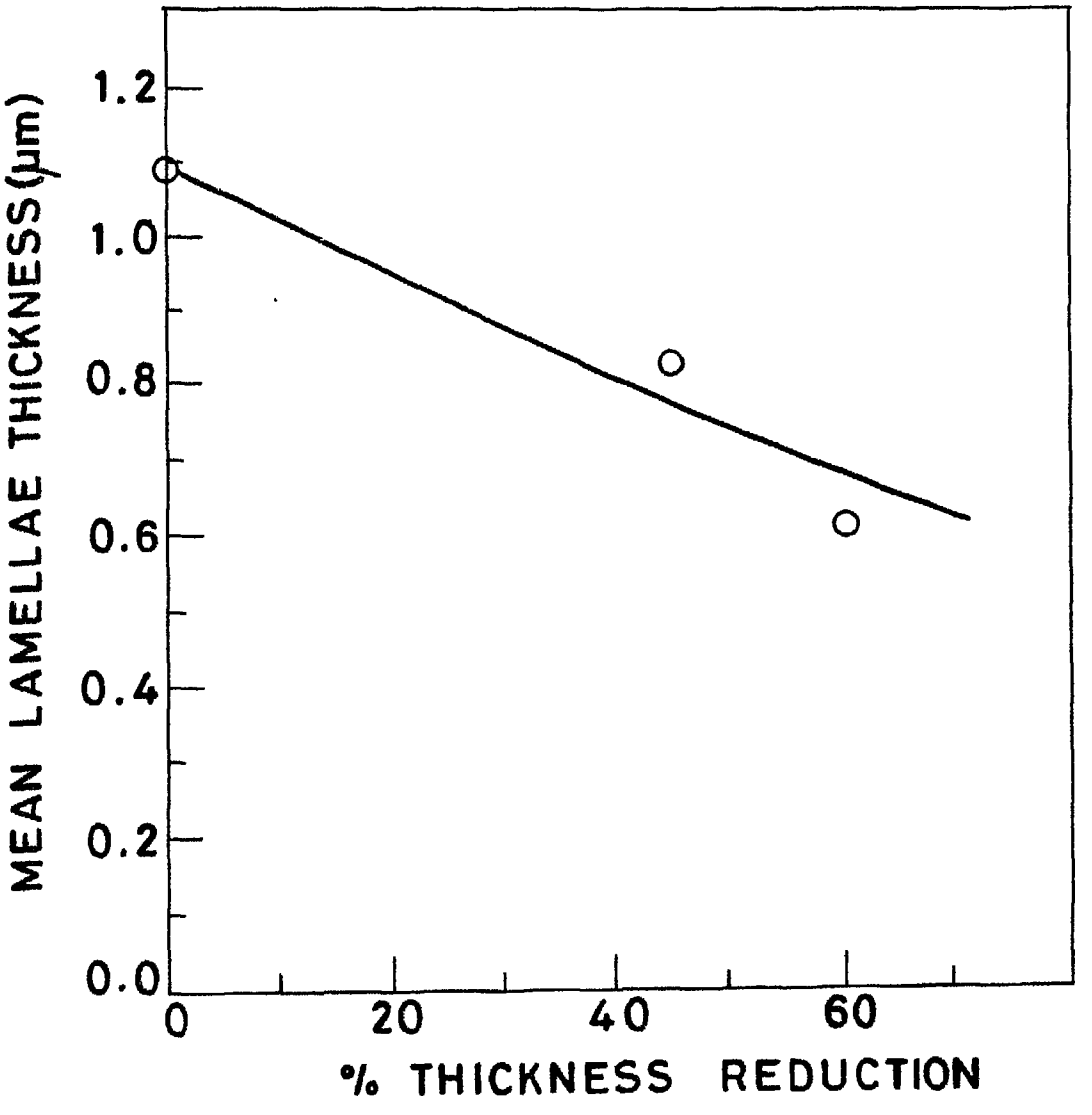

Fig.3.3 Variation of mean lamellae thickness with % thickness reduction at 950°C.

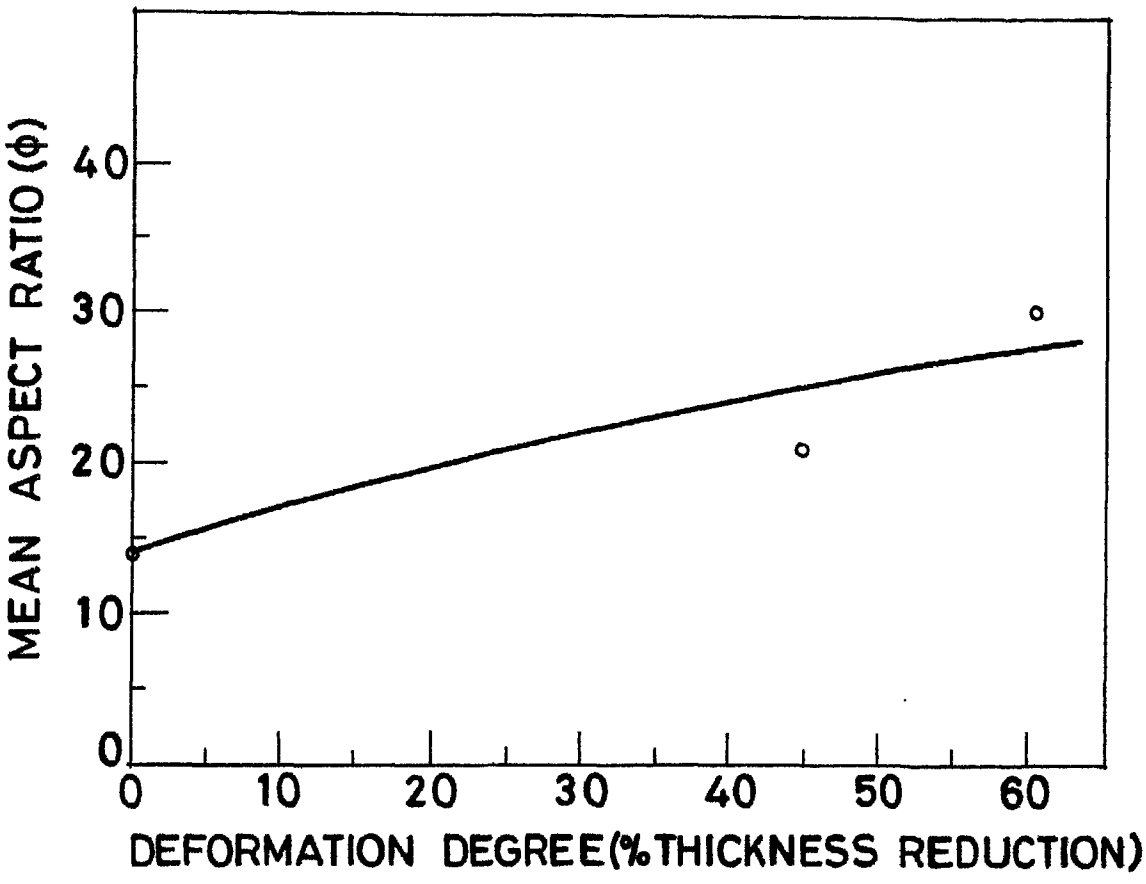

Fig·3.5 Effect of degree of deformation on the mean aspect ratio of the alpha lamellae in samples hot rolled at 950°C.

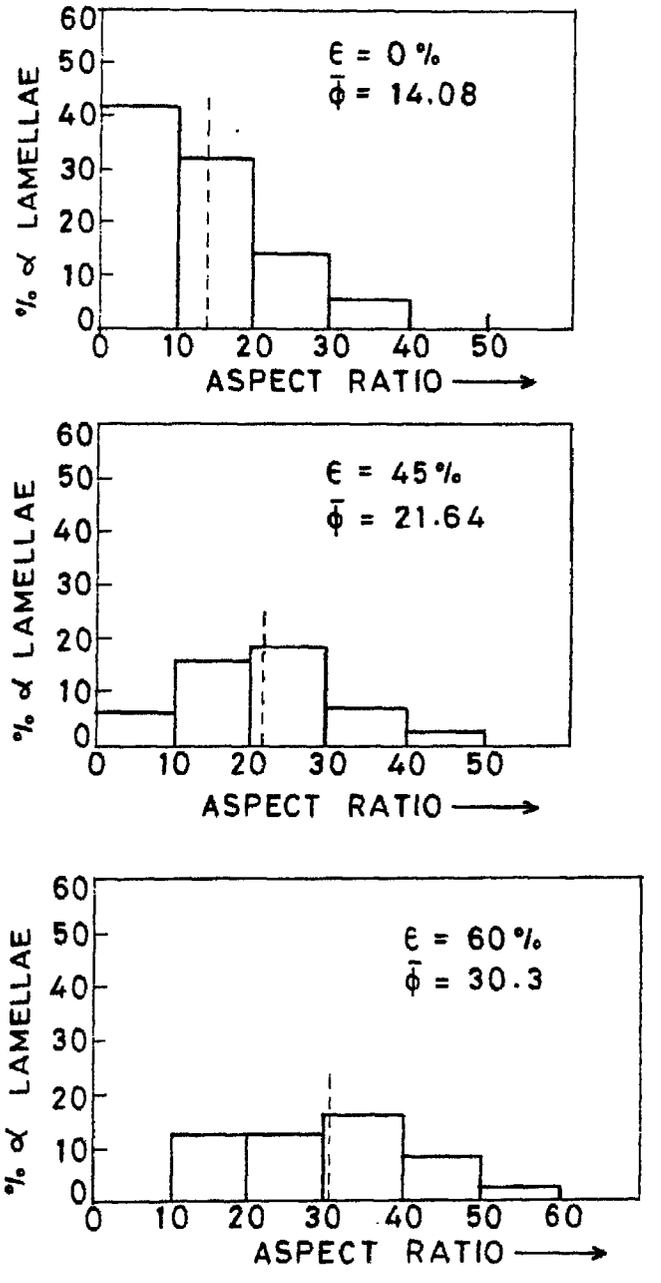

Fig.3.4 Effect of degree of deformation on the aspect ratio distribution of alpha lamellae.
Temperature of deformation =950°C.

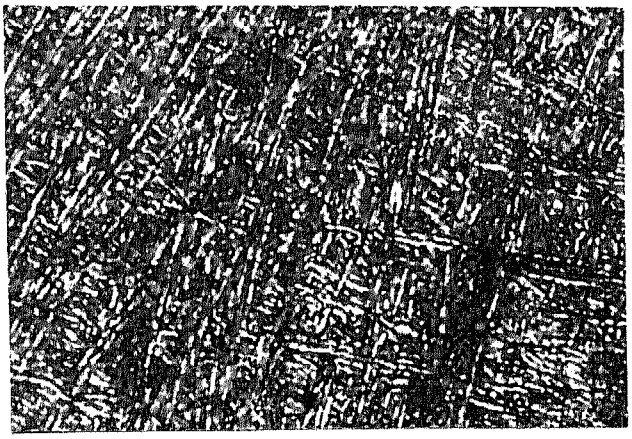

1000 X

a

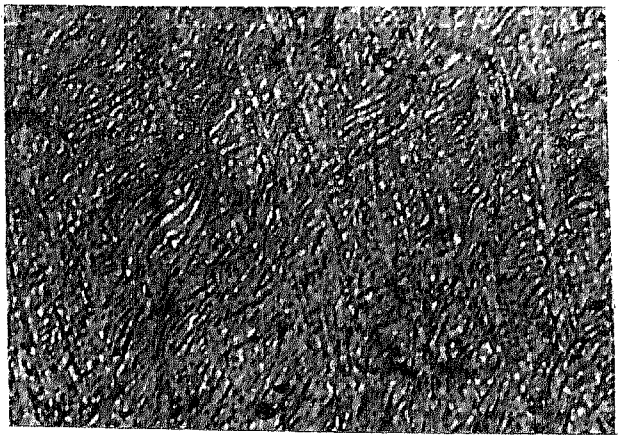

1000X

b

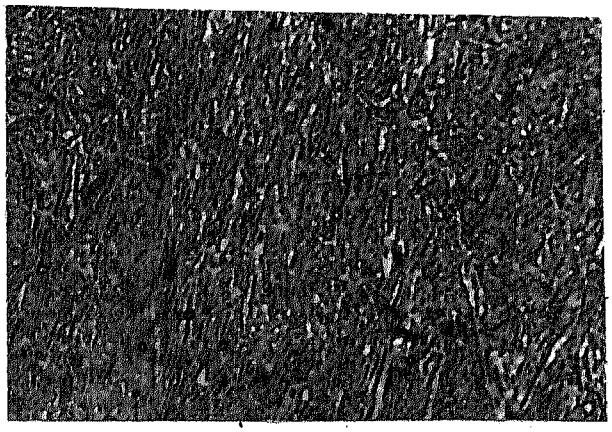

1000 X

c

Fig. 3.6 Microstructures of samples rolled at 850°C with different thickness reductions (a) 20%, (b) 45%, (c) 58%

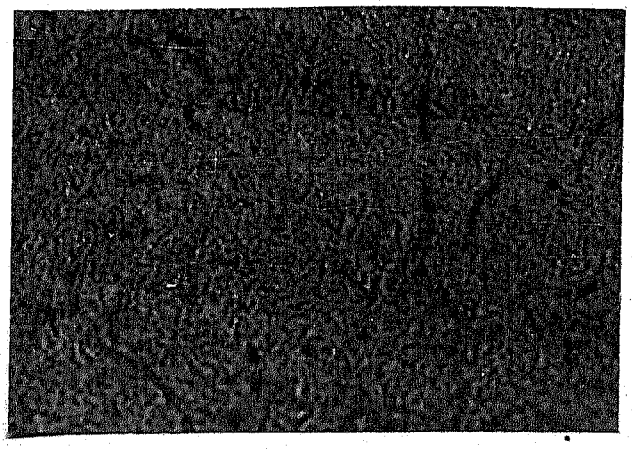

1000 X

a

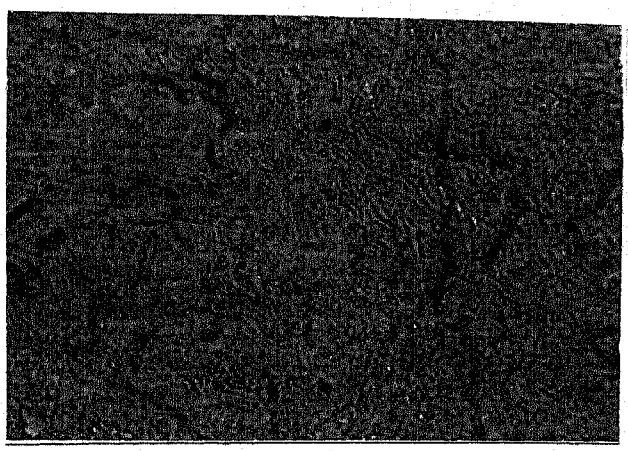

1000 X

b

Fig. 3.7 Microstructures of samples rolled at 750°C with different thickness reductions (a) 47% (b) 68%

deformation temperature was high. But with increasing degree of deformation and lowering of rolling temperature lamellae rotated, sheared and fractured. This process is amplified at 750°C when thermally activated dynamic restoration processes are retarded and short curved lamellae can be seen in samples deformed to 47% unlike at 850°C when it was observable only on deformation to 58%. Due to the fineness of microstructural features, no analysis of aspect ratio of α lamellae and its distribution could be done on samples rolled at 850°C and 750°C.

3.2 Rolling in Single Phase β Field

Deformation in the beta field offers well known technological advantages. In addition, microstructural requirements can be met by properly controlling variables related to deformation and recrystallization. In order to understand the nature of microstructural refinement in β phase field rolling samples were rolled with different thickness reductions at 1050°C. A temperature higher than 40-50°C above the β transus temperature causes coarsening and is likely to offset advantages to be gained by rolling.

Results of the experiments related to rolling in the β phase field indicated that at low thickness reductions the beta grains got elongated along the rolling direction. A higher degree of deformation resulted in the breakdown of grains to more equiaxed morphology with smaller aspect ratios. Figure 3.8 depicts the morphology of the β grains varying with deformation degree. These observations are based on retention of prior β grain boundaries after quenching when β phase transforms to

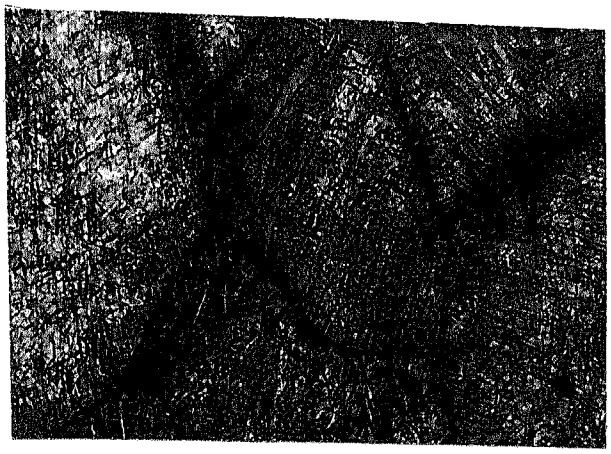

100 X

a

100 X

b

100 X

c

100 X

d

Fig. 3.8 Microstructures of samples rolled at 1050^{0}C with different thickness reductions (a) 20%, (b) 35%, (c) 46% (d) 59%

martensite. Figure 3.9 gives the variation of aspect ratio of β grains with deformation degree.

It is well known that dynamic recovery is the dominant softening mechanism in the deformation of β phase [24,25,30] which manifests itself with the development of a highly recovered substructure from the initial β grains.Quenching after deformation leads to β phase transforming to hexagonal martensite (α') whose length is determined by the size of the subgrains. ince for a particular strain rate irrespective of the strain subgraian size is fixed [5] therefore length of martensite needles will also be fixed for different samples. But as is well known higher dislocation density will lead to greater nucleation centres, therefore martensite needles will be finer with increasing strain as is observed in Figure 3.10.

3.3 Rolling in β Field Folowed by Rolling in (α + β) Field

3.3.1 Effect of Strain in β Field on Starting Microstructure for Rolling in (α + β) Field

Samples were rolled to different strains in the β field (1050^{0}C), annealed at 950^{0}C for 20 min and water quenched. Microstructures of these samples, comprised the starting microstructures prior to rolling in the (α + β) field at 950^{0}C [Figure 3.11]. Figure 3.12 shows changes in the aspect ratio distribution obtained at different strains. With increasing degree of deformation aspect ratio of lamellae shifts to smaller values leading to reduction in mean aspect ratio. Plot of mean aspect ratio with deformation degree is therefore downward sloping (Figure 3.13).

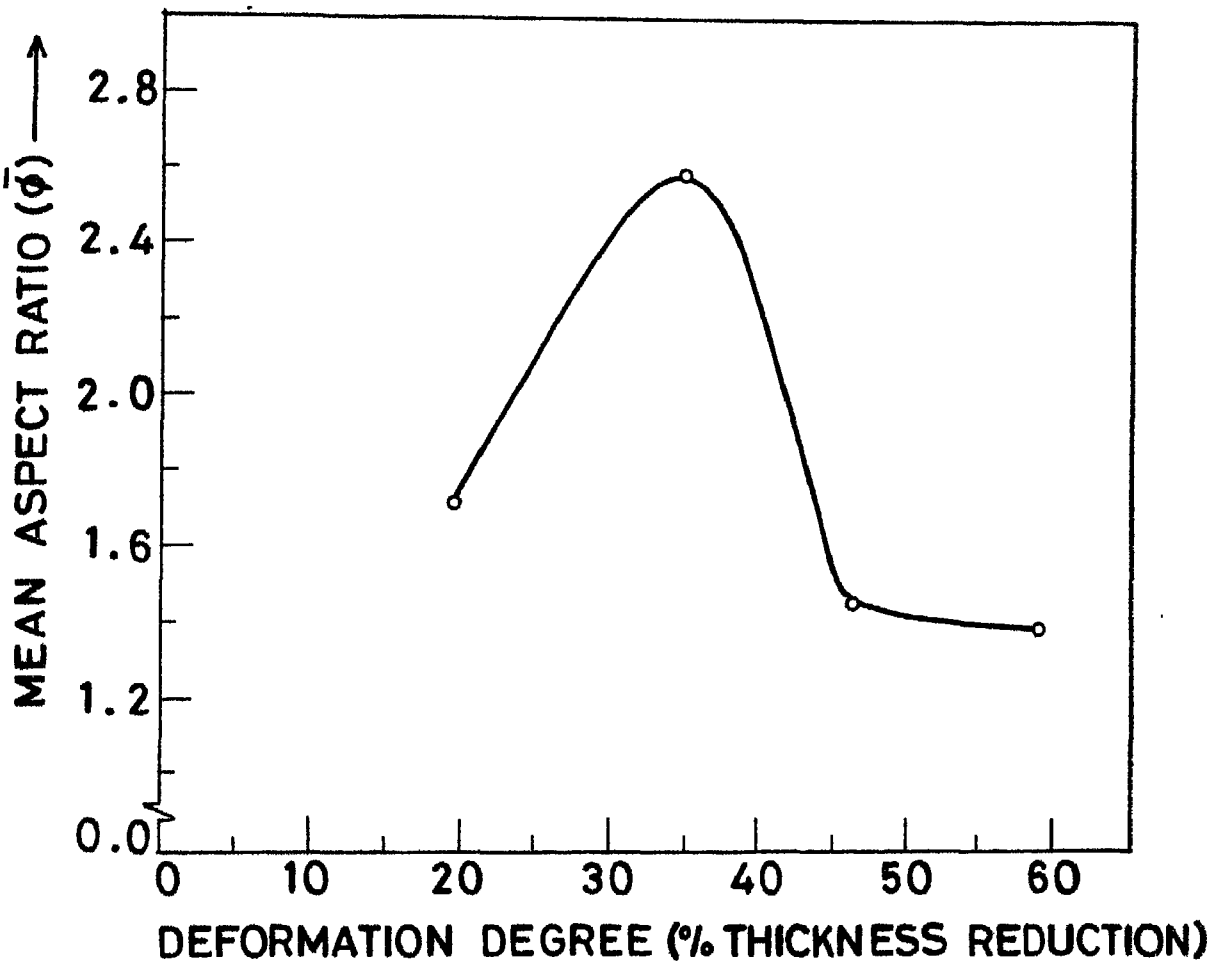

Fig.3.9 The effect of deformation degree on the mean aspect ratio of beta phase. Temperature of deformation =1050°C.

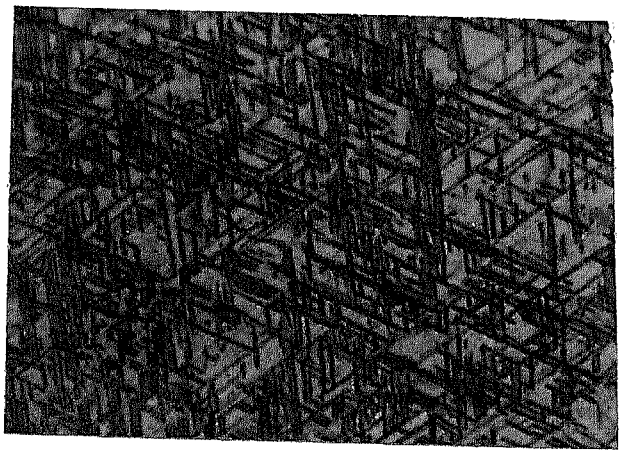

1000 X

a

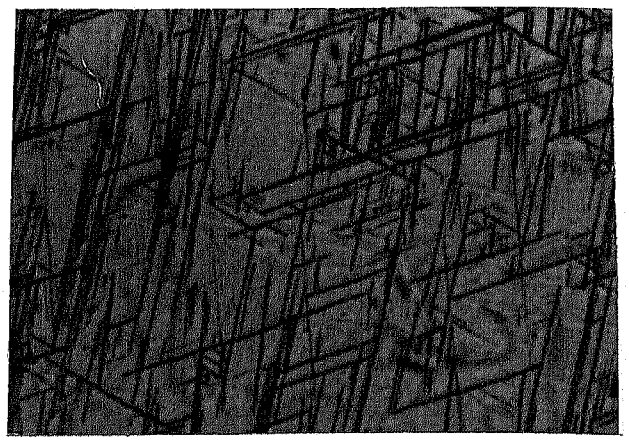

1000 X

b.

Fig. 3.10 Microstructures of samples rolled at 1050°C with thickness reductions of (a) 20% (b) 35%

1000 x

à

1000 x

b

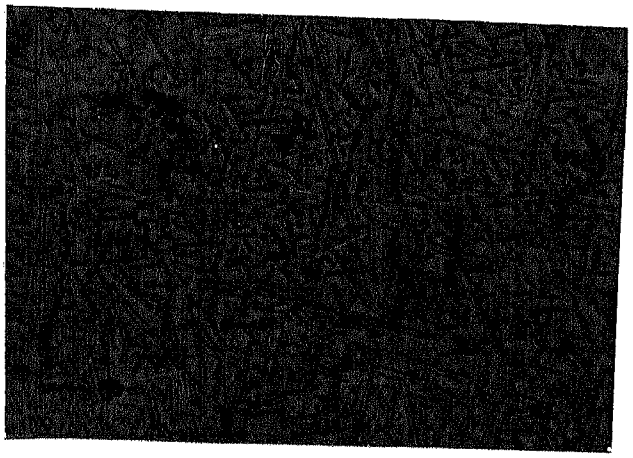

500 x

c

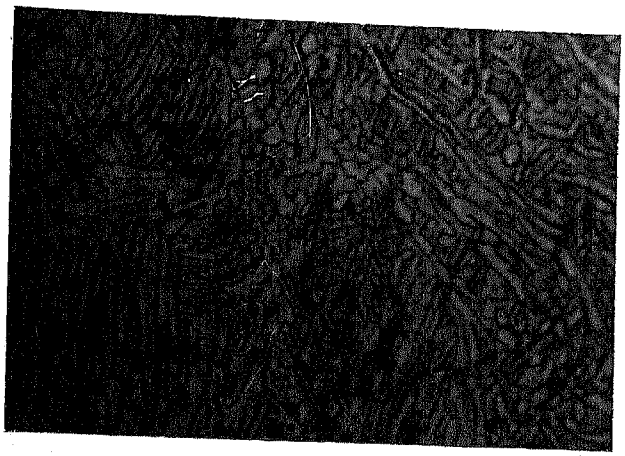

1000 x

d

Fig. 3.11 Microstructures of samples rolled at 1050°C with different thickness reductions and recrystallized at 950°C for 20 min (a) 20% (b) 35% (c) 46% (d) 59%

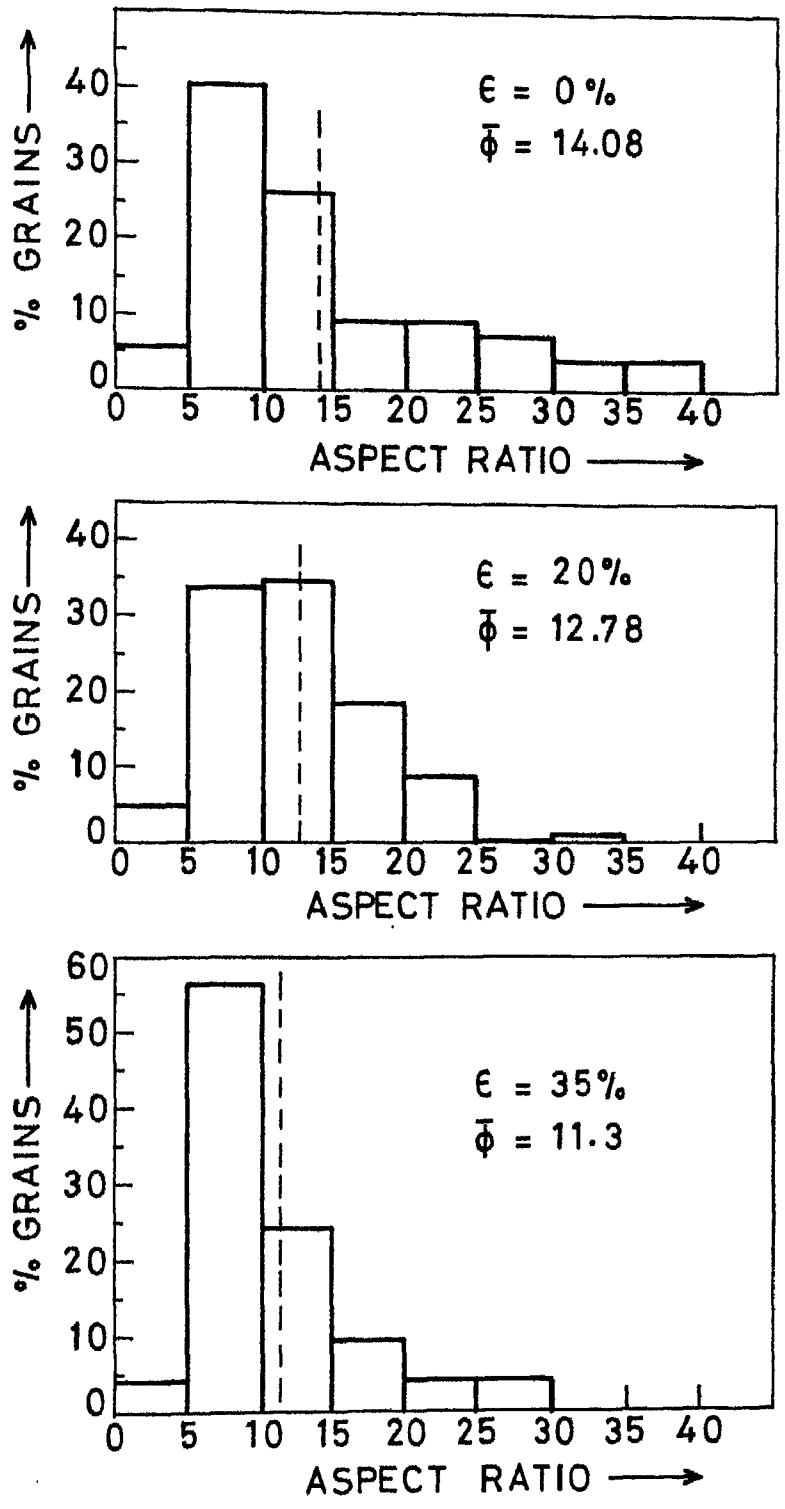

Fig·3.12 (continued)

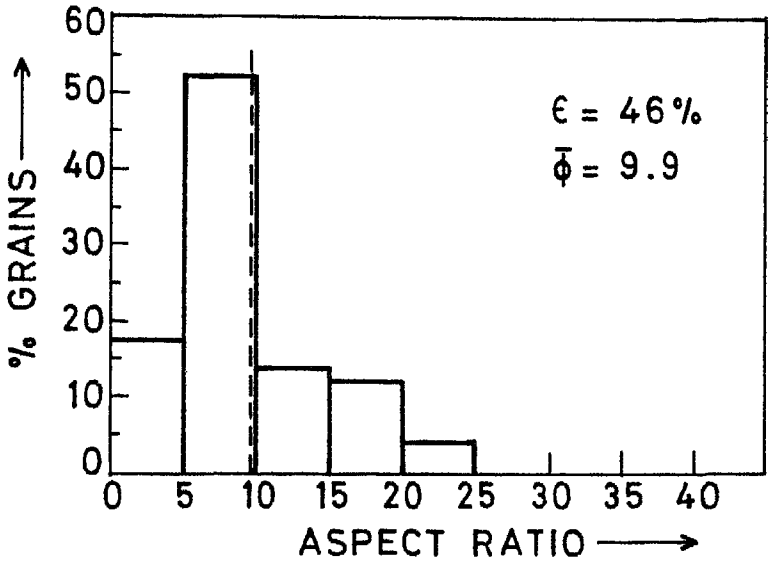

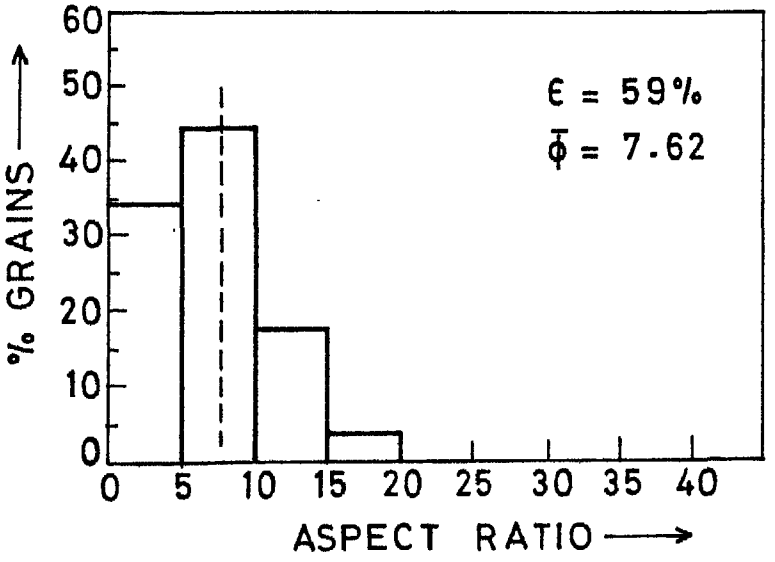

Fig.3.12 Aspect ratio distribution of alpha grains at different strains in beta field.
Temperature of deformation=1050°C.
Annealing temperature =950°C.
Annealing time = 20 min.

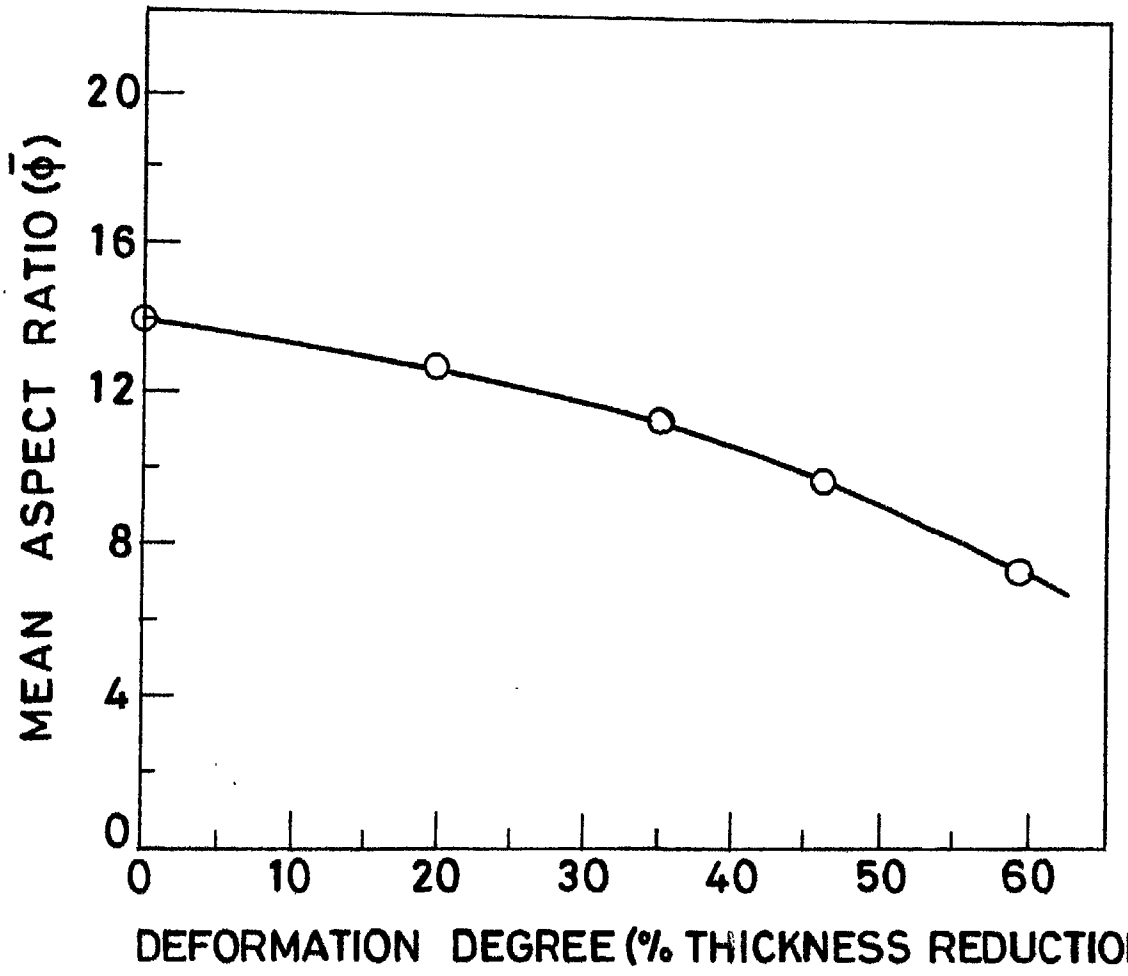

Fig.3.13 Effect of deformation degree in the beta field on the mean aspect ratio of the alpha phase.
Temperature of deformation = 1050°C.
Temperature of recrystallization = 950°C.
Time of recrystallization = 20 min.

As discussed in Section 3.2 increasing the degree of deformation in the beta field leads to increasingly finer masrtensitic needles which on recrystallization give rise to finer alpha lamellae. As is well known finer lamellar break up faster to give size to smaller aspect ratio alpha grains [19,22]. Thus with the same annealing time microstructure of samples rolled to higher strains will show greater percentage of alpha having smaller aspect ratios [Figure 3.11(a) and Figure 3.11(d)]. Higher strains also result in larger stored energies resulting in accelerated recrystallization kinetics. This will be true for starting microstructure at any temperature (besides 950^{0}C which is considered here) though at lower temperatures fraction of low aspect ratio alpha will be lesser since recrystallization is a thermally activated process.

3.3.2 Effect of Strain Ratio in β and (α + β) Fields Keeping Total Strain Fixed on Resulting Microstructure

Figure 3.14 shows microstructure of samples deformed with different strain ratios at 1050^{0}C and 850^{0}C keeping total strain fixed. Microstructure of sample deformed with thickness reduction 22% at 1050^{0}C followed by 36% thickness reduction at 850^{0}C [Figure 3.14(a)] shows short fine lamellae with low aspect ratios in contrast to relatively coarser lamellae observed in Figure 3.14(b) for sample deformed 40% with thickness reduction at 1050^{0}C followed by 15% thickness reduction at 850^{0}C. Strain ratio is therefore an important parameter affecting microstructure evolution.

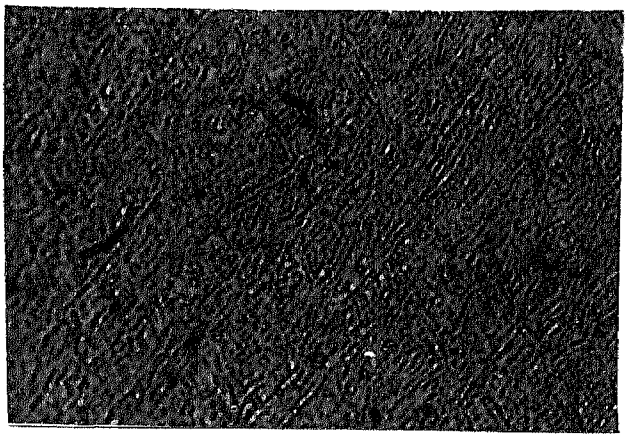

1000 X

a

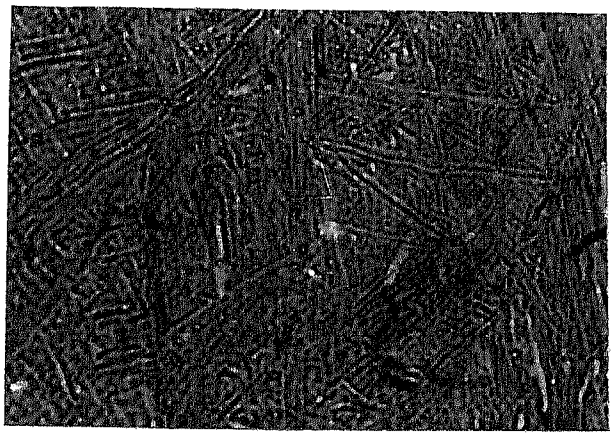

1000 X

b

Fig. 3.14 Microstructures of samples deformed with different strain ratios in the β field (1050^{o}C) and (α + β) field (850^{o}C) (a) 22% 1050^{o}C , 36% 850^{o}C (b) 40% 1050^{o}C, 15% 850^{o}C

3.4 Recrystallization of As Rolled Samples

3.4.1 Recrystallization of Samples Rolled in the ($\alpha + \beta$) Two Phase Region

All the rolled samples were recrystallized at 800°C for 1 hr and 12 hrs. The temperature chosen was such as to be different from the deformation temperatures of 750°C, 850°C and 950°C which caused volume changes facilitating conversion of high aspect ratio alpha lamellae to equiaxed or low aspect ratio alpha grain.

(a) Effect of Temperature:

Comparison of microstructure on recrystallization, after deformation to same degree at different temperatures reveals a reduction in degree of recrystallization with increasing temperature. Higher temperatures cause greater reduction in dislocation density driving force for static recrystallization due to the accelerated dynamic recovery and recrystallization processes operative at such temperatures thereby explaining the observations.

Microstructure of sample rolled with 45% thickness reduction at 950°C shows predominantly lamellae structure on recrystallization [Figure 3.15(a)] while the one rolled at 750°C with same degree of deformation on recrystallization shows small equiaxed grains of size 1.05 μm [Figure 3.15(c)]. Sample rolled at 850°C shows a mixed microstructure with both type of constituents - lamellar as well as equiaxed alpha [Figure 3.15(b)]. Thin foil micrograph of sample rolled 20% and

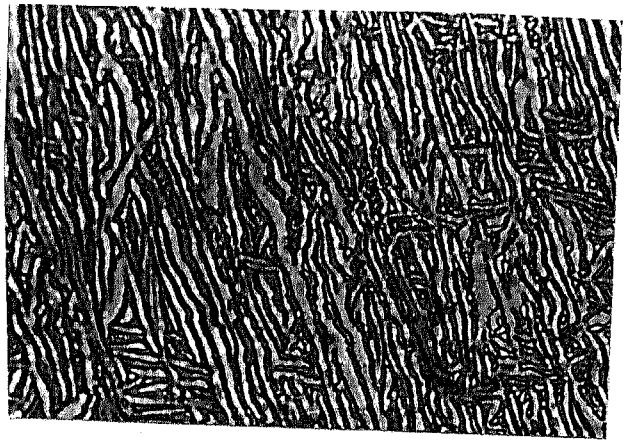

1000 X

a

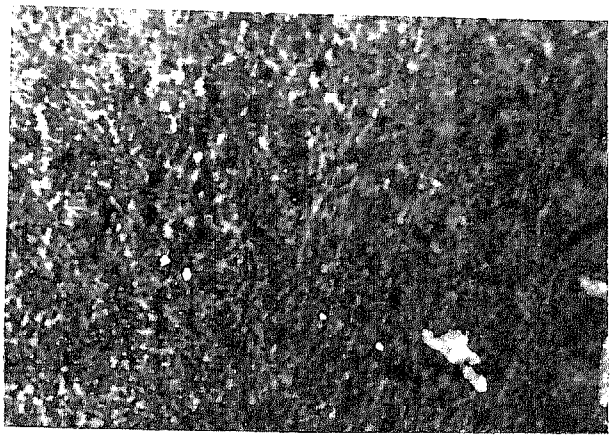

1000 X

b

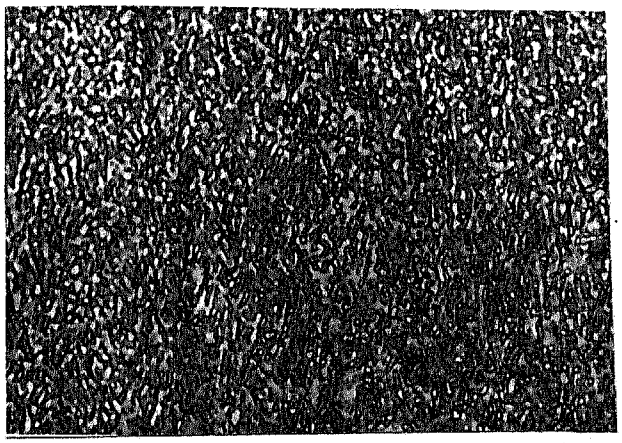

1000 X

c

Fig. 3.15 Microstructures of samples rolled with 45% thickness reduction at different temperatures and annealed for 1 hr at 800^{0}C

(a) 950^{0}C, (b) 850^{0}C and (c) 750^{0}C

recrystallized for 1 hr [Figure 3.16(a)] shows lamellar alpha with large of twins inside it. Small equiaxed grains are also observed at certain locations. Figure [3.16(b)] shows β phase penetrating through the α lamellae.

When recrystallized for 12 hours thin foil micrograph shows large equiaxed β grains with broken down remnants of α lamellae [Figure 3.17(a)]. Figure [3.17(b)] shows lamellar α having well developed internal substructure inside. Subgrains have low wall thickness. Observation of the lamellae at higher magnifications [Figure 3.17(c)] shows little dislocation density inside but stacking faults are observed at certain locations.

(b) Effect of Strain

Increase in strain (thickness reduction) leads to increase in residual stored energy at all temperatures resulting in both accelerated kinetics as well as increasing degree of recrystallization. As a consequence the volume fraction of equiaxed alpha increases [Figure 3.18(a) and 3.15(a)] and Figure [3.18(b) and Figure 3.18(c)] while greater nucleation centres reduce its size [Figure 3.15(c) and Figure 3.18(d)].

(c) Annealing Time

Increasing the annealing time results in completion of recrystallization process along with increase in alpha grain size due to coarsening. Figure 3.19 shows microstructure of samples annealed for 12 hrs after being rolled 60% at 950^0C, 68% at 750^0C and 58% at 850^0C respectively. Table 3.1 gives the grain sizes

33000 X

a

26000 X

b

Fig. 3.16 Thin foil micrographs of samples rolled with 20% thickness reduction at 850°C and annealed for 1 hr at 800°C

a 16000 X

b 20000 X

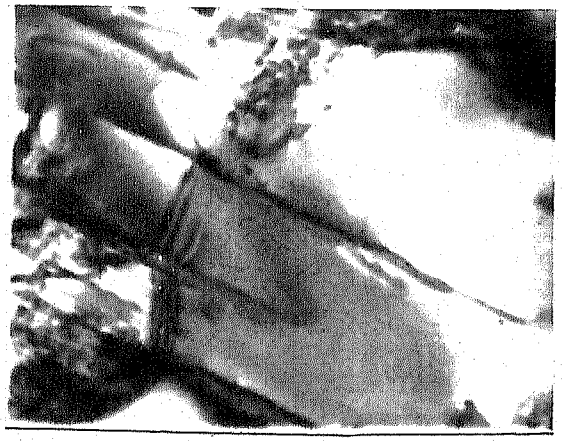

c 24000 X

Fig. 3.17 Thin foil micrographs of samples rolled with 20% thickness reduction at 850°C and annealed for 12 hrs at 800°C

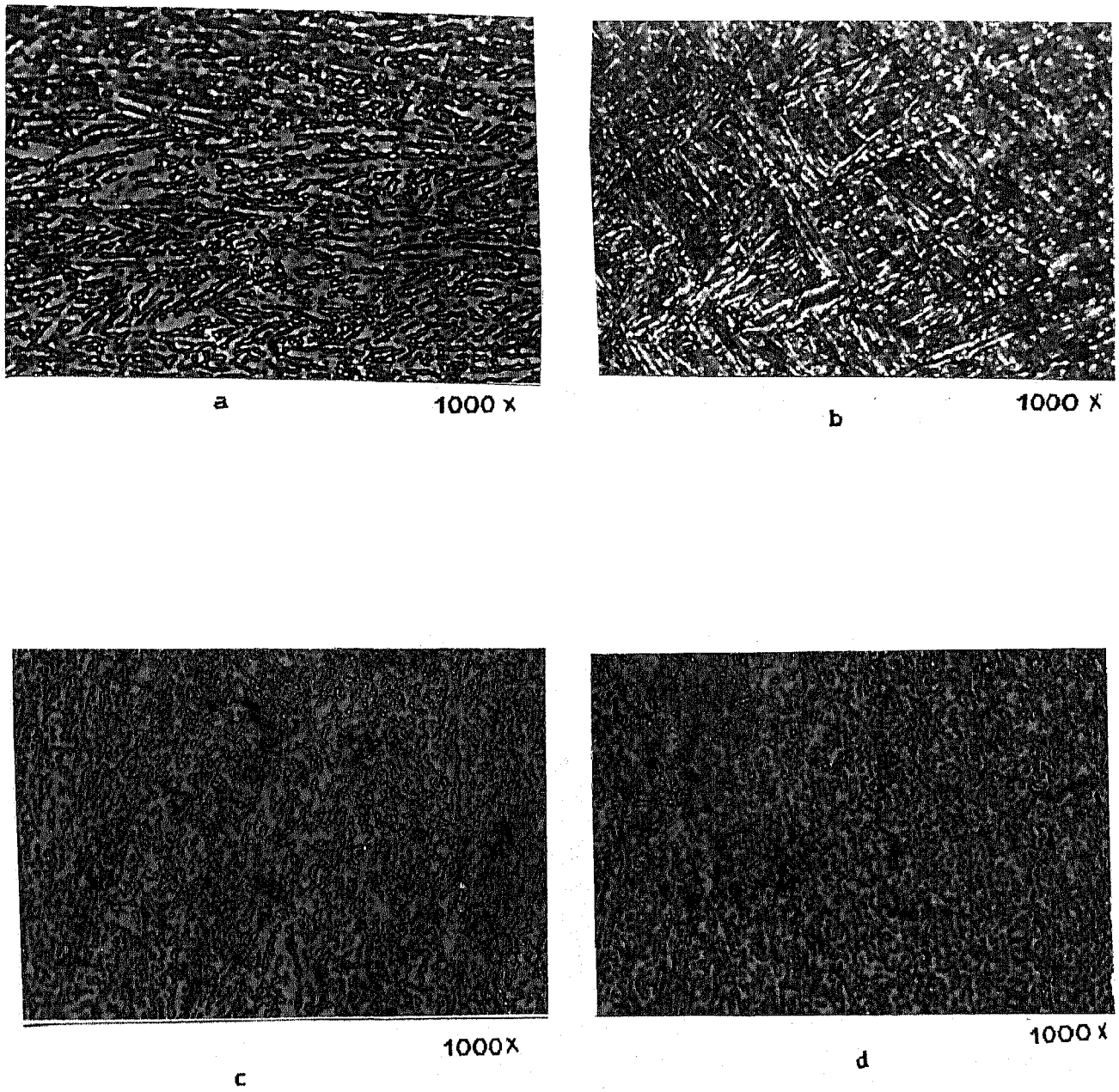

Fig.3.18 Microstructures of samples rolled with different thickness reductions at different temperatures and annealed for1 hr at 800^{0}C

(a) 60% 950^{0}C, (b) 20% 850^{0}C

(c) 58% 850^{0}C, (d) 68% 750^{0}C

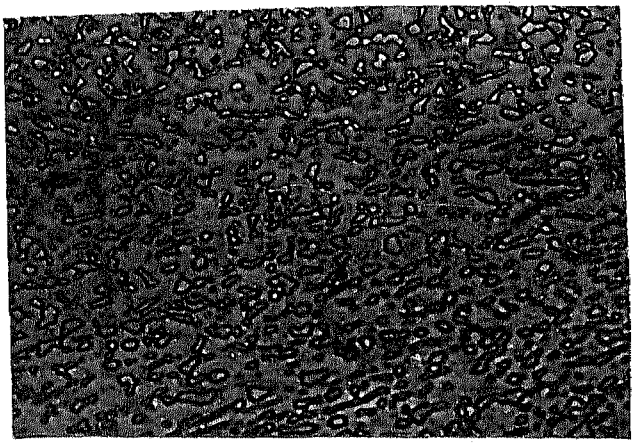

a 1000X

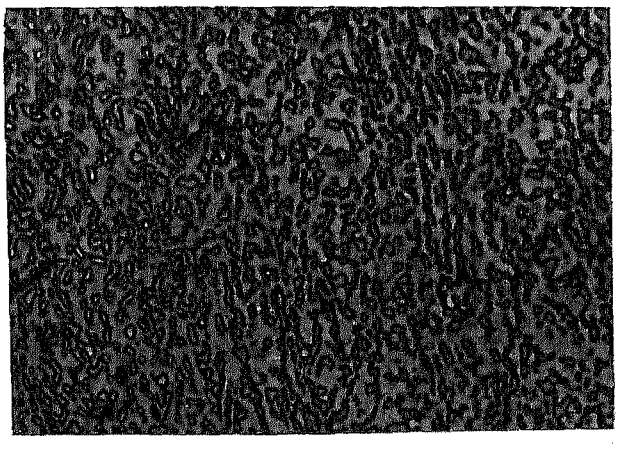

b 1000X

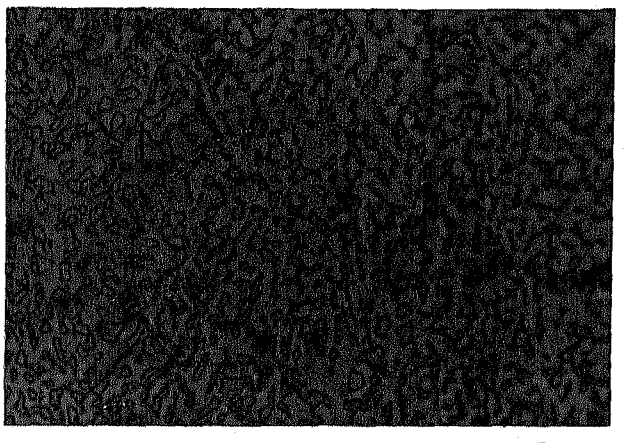

c 1000X

Fig. 3.19 Microstructures of samples annealed for 12 hrs at 800^{0}C after being rolled to different strains at different temperatures

(a) 60% 950^{0}C, (b) 68% 750^{0}C

(c) 58% 850^{0}C

Table 3.1

Rolling temperature (^{o}C)	Degree of deformation (% thickness reduction)	Aspect ratio/grain size after recrystallization for 1 hr	Aspect ratio/ grain size after recrystallization for 12 hrs
950^{o}C	45	--	2.37
	60	--	2.40 μm
850^{o}C	20	--	
	45	--	2.00 μm
	58	1.09 μm	2.20μm
750^{o}C	47	1.05 μm	1.27 μm
	68	0.99 μm	1.90μm

Note: Values are not given for mixed type of microstructure, i.e. where both lamellae are equiaxed constituents are present

or aspect ratios for different samples after recrystallization for 1 hr and 12 hrs.

3.4.2 Recrystallization of Samples Rolled in the β Phase Field

Samples were annealed at 800°C for 1 hr and 12 hrs for recrystallization. Microstructure shows increasing volume fraction of equiaxed alpha with increasing strain [Figure 3.20] though it was considerably lesser when compared with samples deformed to equivalent thickness reductions at lower temperatures. As discussed earlier this is because of greater dislocation annihilation at higher temperatures.

Annealing for 12 hr has the same effect as that for samples deformed at lower temperature in the (α + β) phase field, i.e. recrystallization is completed and coarsening of both alpha plates as well as equiaxed alpha takes place [Figure 3.21].

3.4.3 Recrystallization of Samples Rolled in the β and (α+β) Fields

Strain ratio in the β and (α + β)fields affects microstructural evolution during annealing. Sample deformed 21% at 1050°C followed by 36% at 850°C on recrystallization shows equiaxed microstructure with alpha grain size 1.63 μm which coarsened negligibly to 1.793 μm on recrystallization for 12 hrs (Figure 3.22). Microstructure compares favourably with that of sample deformed 58% at 850°C and recrystallized for 1 hr though alpha given size in the latter case is slightly lesser (1.09 μm). Thus with the same strain but part of it being

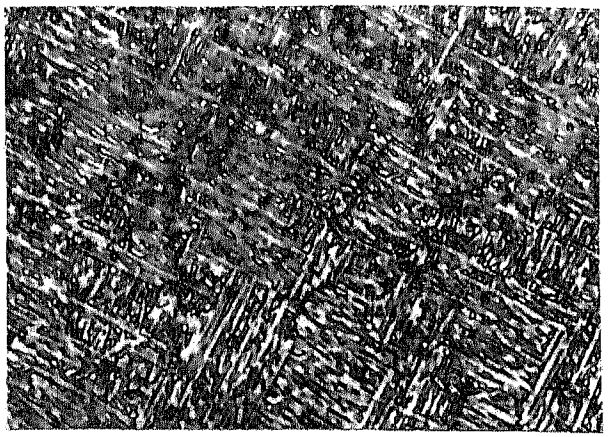

1000 X

a

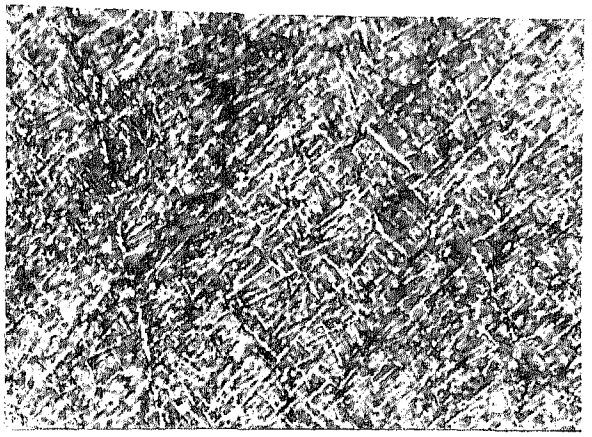

1000 X

b

1000 X

c

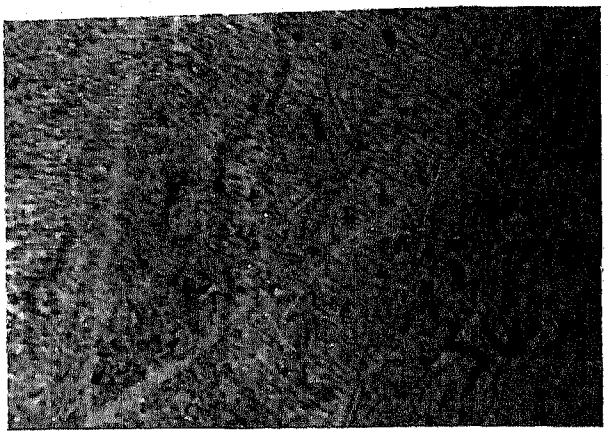

1000 X

d

Fig. 3.20 Microstructures of samples deformed with different thickness reductions at 1050^{0}C and annealed at 800^{0}C for 1 hr(a) 20% (b) 35% (c) 46% (d) 59%

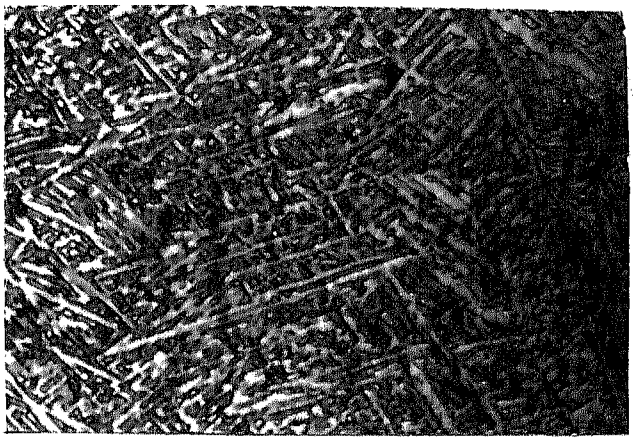

1000 X

a

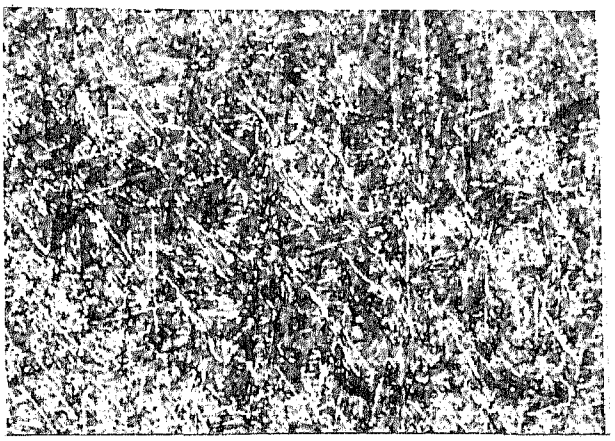

1000 X

b

1000 X

c

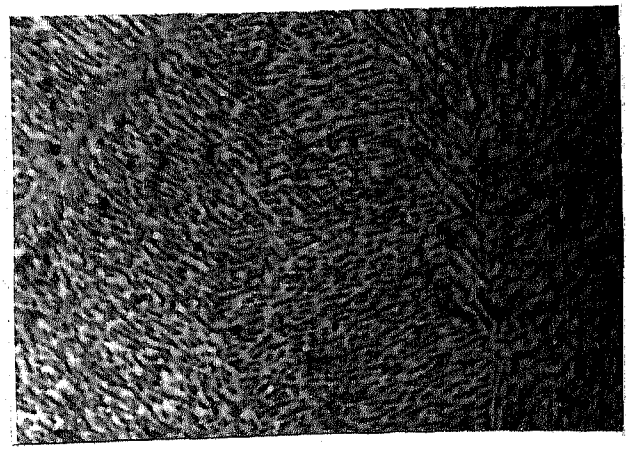

1000 X

d

Fig. 3.21 Microstructures of samples deformed with different thickness reduction at 1050^{o}C and annealed at 800^{o}C for 12 hrs (a) 20% (b) 35% (c) 46% (d) 59%

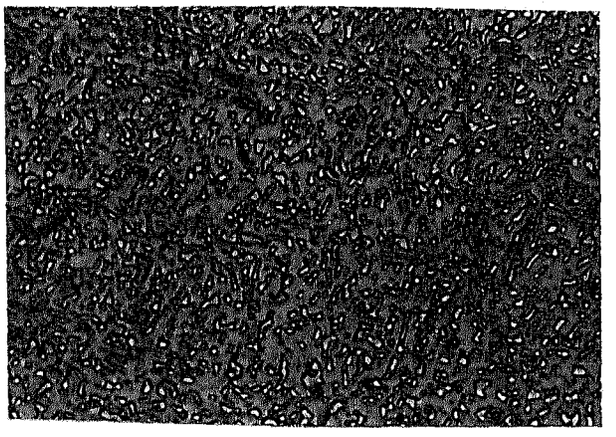

a 1000 X

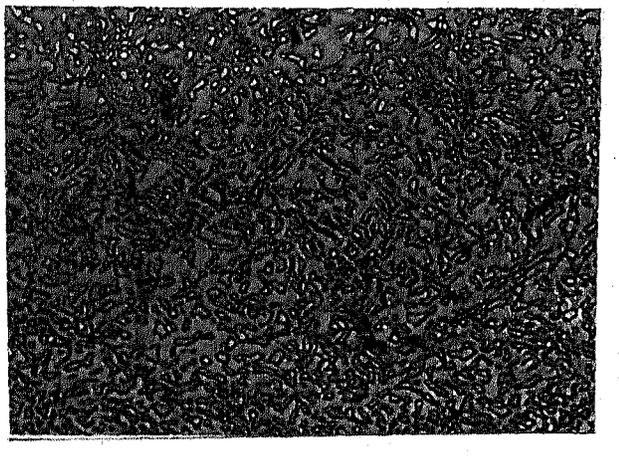

b 1000 X

Fig. 3.22 Microstructures of samples rolled 22% at 1050^{0}C and 36% at 850^{0}C after annealing at 800^{0}C for different times

(a) 1 hr, (b) 12 hrs

imparted in the β field it was possible to generate equiaxed microstructure similar to when sample was deformed entirely in the two phase (α + β) field. Essential prerequisite is optimisation of deformation in beta field since it is observed that higher deformation degree in the β field on recrystallization for 1 hr resulted in lamellar microstructure being maintained (Figure 3.23). Recrystallization for 12 hrs although lead to break up of the lamellae but aspect ratio was still high.

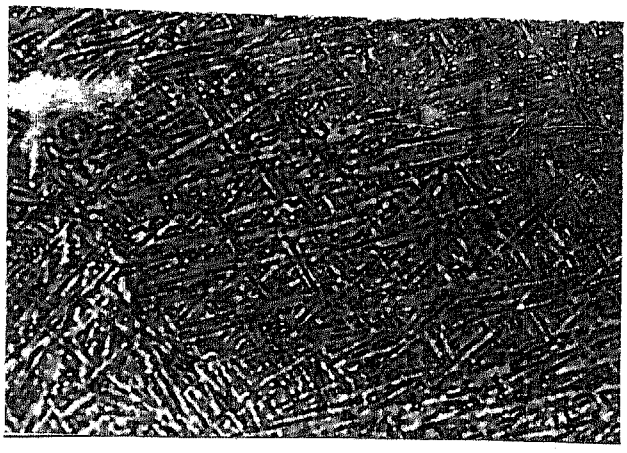

1000 X

a

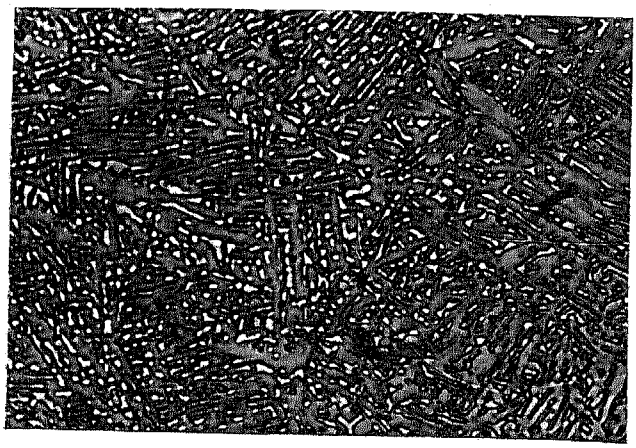

1000 X

b

Fig. 3.23 Microstructures of samples rolled 40% and 1050°C and 15% at 850°C after annealing at 800°C for different times

(a) 1 hr, (b) 12 hrs.

CHAPTER 4

CONCLUSIONS AND SUGGESTIONS FOR FURTHER STUDY

4.1 Conclusions

1. A new method based on evolving equiaxed α morphology in Ti-632Si alloy by thermomechanical treatment of fine lamellar structure, obtained by ageing the β quenched microstructure, has been successfully tried. This approach is in contrast to the traditional method of obtaining the equiaxed α by the thermomechanical working of the initial Widmanstatten structure. Equiaxed α grains as small as 1 μm were generated by hot rolling followed by recrystallization annealing.

2. Hot rolling strain, rolling temperature, annealing time, and lamellae thickness were found to affect the evolution of equiaxed morphology of α phase in Ti-632Si alloy.

3. Investigation into the nature of deformation of lamellar structure in (α+β) field revealed that while at lower temperature lamellae get sheared and fracture easily , at higher temperature they show high ductility. Aspect ratio increases with increasing strain (length increases and thickness decreases) for the latter case.

4. Higher hot rolling strains and lower deformation temperatures in ($\alpha+\beta$) field resulted in smaller grain sizes of recrystallized α possibly due to the accelerated recrystallization kinetics. Larger annealing times resulted in coarsening with consequent increase in grain sizes. Finer lamellae were found to convert more easily to equiaxed structure than coarse lamellae.

5. Deformation in the β field resulted in elongation followed by breakup of β grains into more equiaxed morphology at higher strains. On recrystallization, α lamellae were formed whose aspect ratio was found to decrase with increasing strain .

6. Based on the above observations a limited number of experiments were conducted involving a new deformation schedule by carrying out rolling in the β and ($\alpha+\beta$) fields in succession. It was found that equiaxed microstructures can be generated by giving a lower strain in the ($\alpha+\beta$) field by such an operation. However, a more exhaustive study is necessary to optimize the degree of deformation in each phase field.

4.2 Suggestions for further work

1. TEM investigations should be done to study the deformation behaviour in different phase fields vis-a-vis its affect on evolution of equiaxad

morphology.

2. Effect of equiaxed morphology , evolved by different routes on mechanical properties should be investigated.

REFERENCES

1. Titanium. A Technical Guide, Matthew J. Donachie. Jr., ASM, 1988.
2. J.B. Borradaile and R.H. Jeal, Titanium Science and Technology'80, Kyoto, Japan, pp. 141.
3. S.M.L. Sastry et al. Titanium Science and Technology'80, Kyoto, Japan, pp. 873.
4. J.C. Chesnutt, C.G. Rhodes and J.C. Williams, Fractography - Microscopy Cracking Processes, ASTM 1976, pp. 99-138.
5. J.C. Williams and E.A. Starke, Jr. Deformation, Processing and Structure, G. Krauss, ed. ASM, Metals Park, Ohio, 1984, pp. 279-354.
6. H. Margolin, J.C. Williams, J.C. Chesnutt and G. Luetjering, Titanium Science and Technology, Kyoto, Japan, pp.169.
7. T.L. Trenogina and R.M. Lerinman, Proc. of 3rd International Conference on Titanium, Moscow, 1976, pp. 1623-1632.
8. J.C. Williams, Titanium Science and Technology, Plenum Press, New York, Vol. 3 1973, pp. 1433.
9. R.I. Jaffee, Titanium Science and Technology, Plenum Press, New York, Vol. 3, 1973, pp. 1665.
10. D.M. Rogers, ibid, pp. 1719.
11. M.J. Blaccrvrn, ibid, pp. 2577.
12. M. Peters and G. Luetjering, Titanium Science and Technology, 1980, Kyoto, Japan,pp. 925.
13. J.C. Williams and G. Luetjering, Titanium '80 Science and

Technology, AIME, New York, Vol. 180, pp. 671.

14. K. Gaziogler, K.J. Grundhoff and P. Fuwke and W. Bunk, Z. Metallkd, 67 (1976). pp. 209.
15. J.J. Lucas, Titanium Science and Technology, Plenum Press, New York, Vol. 3 (1973) pp. 2081.
16. C.A. Stubbington and A.W. Bowen, J. Mat. Science, 9, 1974, pp. 941.
17. Shakhanova et al., Titanium Science and Tech. '80, Kyoto, Japan, pp. 849.
18. K. Morii, H. Mecking and G. Luetjering, Proc. of Int. Conf. on Strength of Metals and Alloys, Pergamon Press, New York (1985), pp. 251.
19. I. Weiss, F.H. Froes, D. Eylon, G.E. Welsch, Vol. 17A, Met. Trans. In Nov., 1986, pp. 1935.
20. Hirosuke Inagaki, Z. Metallkd, Aug. 1990, pp. 540.
21. H. Margolin and Paul Cohen, Titanium Science and Tech.'80, Kyoto, Japan, pp. 1565.
22. M. Peters, G. Luetjering and Ziegler, Z. Metallka, May 1983, pp. 274-282.
23. H.J. McQueen and J.J. Jonas : Treatise on Materials Science and Tech. Plastic Deformation of Materials, R.J. Arsenault ed. Academic Press, New York, 1975, Vol. 6, pp. 393.
24. T. Sheppard and J. Norley, Material Sci. & Tech., Oct. 88.
25. R.M. Lerinman, T.L. Trenogina and O.A. Yolkina, Proc. of 3rd Int. Conf. on Titanium, Moscow, 76, pp. 1809.
26. C.C. Chen and J.E. Coyne, Met. Trans. 78, 1976, p. 1931.
27. S.L. Semiatin and G.D. Lahoti, Met. Tran 1981, pp. 1705.
28. C.J. McHargue and J.P. Hammond, J. Met. 57, Jan. 1953.

29. Nishimura et al., Tit. Sci. & Tech. 80, Kyoto, Japan, pp. 937.

30. D. Bourell and H.J. McQueen: J. Appl. Metal Work, 1987, Vol. 5, pp. 53-73.

31. M.J. Blackburn and J.C. Williams, Trans. TMS AIME., 1967 Vol. 239, pp. 287-288.